On Updating Static Output Feedback Controllers Under State-Space Perturbation

MirSaleh Bahavarnia† and Ahmad F. Taha†

***Abstract*—In this paper, we propose a novel update of a nominal stabilizing static output feedback (SOF) controller for a perturbed linear system. In almost every classical feedback controller design problem, a stabilizing feedback controller is designed given a stabilizable unstable system. In realistic scenarios, the system model is usually imperfect and subject to *perturbations*. A typical approach to attenuate the impacts of such perturbations on the system stability is repeating the whole controller design procedure to find an updated stabilizing SOF controller. Such an approach can be inefficient and occasionally infeasible. Using the notion of *minimum destabilizing real perturbation* (MDRP), we construct a simple norm minimization problem (a least-squares problem) to propose an efficient update of a nominal stabilizing SOF controller that can be applied to various control engineering applications in the case of perturbed scenarios like abrupt changes or inaccurate system models. In particular, considering norm-bounded known or unknown perturbations, this paper presents updated stabilizing SOF controllers and derives sufficient stability conditions. Geometric metrics to quantitatively measure the approach's robustness are defined. Moreover, we characterize the corresponding guaranteed stability regions and specifically, for the case of norm-bounded unknown perturbations, we propose non-fragility-based robust updated stabilizing SOF controllers. Through extensive numerical simulations, we assess the effectiveness of the theoretical results.**

***Index Terms*—Stability of linear systems, robust control, output feedback control, uncertain linear systems.**

I. Introduction

STABILITY robustness is a significant classical notion in robust control theory [1]–[8]. Stability robustness simply means how sensitive the stability of the control system is against the perturbations/uncertainties. The varying nature of engineering systems' models necessitates the thorough analysis of stability robustness and its potential applications to develop robustly stable engineering systems. Several studies have quantitatively investigated the impacts of perturbations on the stability robustness of the control systems. In [1], [3], a class of non-destabilizing linear constant perturbations is characterized for the linear-quadratic state feedback (LQSF) designs. The authors in [2], propose a guaranteed cost LQSF for which the closed-loop system is stable for any variation of a vector-valued parameter. In [4], for the LQSF designs, the stability robustness bounds are derived based on the Algebraic Riccati equation and Lyapunov stability theory. In [5], bounds on the non-destabilizing time-varying nonlinear perturbations are obtained for asymptotically stable linear systems to provide computationally efficient quantitative robustness measures. Various stability robustness tests are investigated in [6] to highlight the trade-off between the stability robustness conservatism and the information about the perturbation. In [7], utilizing the Lyapunov stability theory, the author has proposed an improved non-destabilizing perturbation bound over the bound proposed by [5]. Taking advantage of appropriately chosen coordinate transformations, the authors in [8] have reduced the conservatism of non-destabilizing perturbation bounds proposed by [5], [7].

In this paper, in contrast to the aforementioned studies, we do not go through the derivation of non-destabilizing perturbation bounds. Instead, we mainly focus on attenuating the impacts of perturbations on the system stability via updating a nominal stabilizing static output feedback (SOF) controller. With that in mind, the control problem considered in this paper is an SOF controller *update* problem. In order to put into perspective, it is noteworthy that our considered problem slightly differs from the robust feedback controller design problems for uncertain linear systems (with norm-bounded unknown perturbation) [9]–[12] in the sense that, the robust feedback controller in those problems is robustly stabilizing for all perturbations Δ satisfying $0 < \|\Delta\|_F \leq \rho$ while in our case, the robust updated stabilizing SOF controller is robustly stabilizing for a subset of perturbations Δ satisfying $0 < \|\Delta\|_F \leq \rho$ that will mathematically be characterized. Specifically, the more accurate estimate $\hat{\Delta}$ of a norm-bounded unknown perturbation we have, the more robustly stabilizing updated stabilizing SOF controller we propose.

In general, the SOF controller stabilization problem is known to be an NP-hard problem as it is intrinsically equivalent to solving a bi-linear matrix inequality (BMI) [13]. Then, utilizing a typical approach by repeating the whole controller design procedure can become computationally cumbersome. Also, we avoid utilizing any Lyapunov-based approach as it enforces an extra computational burden (mostly in the case of bi-linear matrix inequality (BMI) or linear matrix inequality (LMI) formulations in semi-definite programs (SDPs) [14]) which is not desired in terms of computational efficiency. It is remarkable that the Lyapunov-based SOF controller synthesis hinges on approximately solving BMIs [15], [16] or incorporating sufficient LMI conditions [12], [17] which induces a conservatism. The alternative non-Lyapunov approach that we take is built upon the notion of *minimum destabilizing real perturbation* [18] which has inspired [19], [20] to synthesize sparse feedback controllers for the large-scale systems. Throughout the paper, we utilize the fundamental

†The authors are with the Department of Civil and Environmental Engineering, Vanderbilt University, 2201 West End Avenue, TN 37235, USA. Ahmad F. Taha is also affiliated with the Department of Electrical and Computer Engineering. Emails: mirsaleh.bahavarnia@vanderbilt.edu, ahmad.taha@vanderbilt.edu.This work is supported by National Science Foundation under Grants 2152450 and 2151571.

linear algebraic results from [21] where needed.

The main contributions of this paper can be itemized as follows:

- Built upon the notion of minimum destabilizing real perturbation [18], we construct a simple norm minimization problem (a least-squares problem) to propose a novel update of a nominal stabilizing SOF controller that can be applied to various control engineering applications in the case of perturbed scenarios like abrupt changes or inaccurate system models.
- Considering known perturbations and unknown perturbations with a known upper bound on their norm, we propose novel updates of nominal stabilizing SOF controllers and derive sufficient stability conditions.
- We define geometric metrics to quantitatively measure the stability robustness of the proposed updates of nominal stabilizing SOF controllers, characterize the corresponding guaranteed stability regions, and specifically, for the case of unknown perturbations with a known upper bound on their norm, we propose non-fragility-based robust updated stabilizing SOF controllers.
- Through extensive numerical simulations, we validate the effectiveness of the theoretical results and present a thorough analysis of the empirical visualizations.

The remainder of the paper is structured as follows: Section II states the main objective of the paper by arising a question to be answered throughout the following sections. Section III presents a novel updated stabilizing SOF controller via updating a nominal stabilizing SOF controller built upon a simple norm minimization problem (a least-squares problem). Section IV contains the main results of the paper detailing the stability regions for the corresponding updated stabilizing SOF controllers. Through various numerical simulations, Section V empirically verifies the effectiveness of the theoretical results. Finally, the paper is concluded via drawing a few concluding remarks in Section VI.

Paper's Notation. We denote the vectors and matrices by lowercase and uppercase letters, respectively. To represent the set of real numbers, n-dimensional real-valued vectors, and $m \times n$-dimensional real-valued matrices, we respectively use $\mathbb{R}$, $\mathbb{R}^n$, and $\mathbb{R}^{m\times n}$. We show the set of positive real numbers with $\mathbb{R}_{++}$. We denote the identity matrix of dimension n with I_n. For a square matrix M, $\alpha(M)$ represents the spectral abscissa (i.e., the maximum real part of the eigenvalues) of M. We say a square matrix M is stable (Hurwitz) if $\alpha(M) < 0$ holds. For a matrix M, symbols M^T, $\|M\|_F$, $\mathbf{vec}(M)$, and $U_M\Sigma_M V_M^T$ denote its transpose, Frobenius norm, vectorization, and singular value decomposition (SVD), respectively. Given a full-column rank matrix M, $M^+ := (M^TM)^{-1}M^T$ denotes the Moore-Penrose inverse of M. We represent the Kronecker product with the symbol $\otimes$. For a vector v, we respectively denote its Euclidean norm and vectorization inverse with $\|v\|$ and $\mathbf{vec}^{-1}(v)$ where $\mathbf{vec}^{-1}(v)$ is a matrix that satisfies $\mathbf{vec}(\mathbf{vec}^{-1}(v)) = v$. We represent the set union with $\cup$. Given two real numbers $a < b$, we denote the open, closed, and half-open intervals with $]a, b[$, $[a, b]$, $[a, b[$, and $]a, b]$, respectively. We represent the logical `or` and the logical `and` with $\vee$ and $\wedge$, respectively. We show the computation complexity with big O notation, i.e., $\mathcal{O}()$. We denote the Gamma function with $\Gamma(.)$. Symbols $\mathcal{U}(0, 1)$ and $\mathcal{N}(0, I)$ respectively represent the uniform distribution on $[0, 1]$ and the normal distribution with zero mean and unit variance.

II. Problem Statement

We consider the following linear state-space model:

$$\dot{x}(t) = (A + BFC)x(t), \tag{1}$$

where $x(t) \in \mathbb{R}^n$, $A \in \mathbb{R}^{n\times n}$, $B \in \mathbb{R}^{n\times m}$, $C \in \mathbb{R}^{p\times n}$, and $F \in \mathbb{R}^{m\times p}$ denote the state vector, state matrix, input matrix, output matrix, and a nominal stabilizing SOF controller matrix (i.e., $\alpha(A + BFC) < 0$ holds), respectively.

Suppose that a norm-bounded perturbation $\Delta \in \mathbb{R}^{n\times n}$ with an upper bound $\rho > 0$ on its Frobenius norm, (i.e., $0 < \|\Delta\|_F \leq \rho$) hits the state-space model (1) as follows:

$$\dot{x}(t) = (A + BFC + \Delta)x(t). \tag{2}$$

On one hand, for non-destabilizing perturbations (e.g., sufficiently small perturbations), although $A + BFC + \Delta$ in (2) is still a stable matrix, the stability robustness can be degraded. On the other hand, for destabilizing perturbations (e.g., more severe perturbations), $A + BFC + \Delta$ in (2) can become unstable. To attenuate the impacts of such perturbations on the stability robustness and the stability, a typical approach can be repeating the whole controller design procedure to find a new SOF controller, namely F^{typical}, to stabilize $A+\Delta$ and get a stable $A + \Delta + BF^{\text{typical}}C$. Such a typical approach can be inefficient in terms of scalability and even infeasible in some cases. Motivated by such an issue and utilizing a simple norm minimization problem (a least-squares problem) built upon the notion of *minimum destabilizing real perturbation* [18], we propose a novel update of a nominal stabilizing SOF controller that can be applied to various control engineering applications in the case of perturbed scenarios like abrupt changes or inaccurate system models.

In a nutshell, the main objective of this paper is to find an answer to the following question:

Q1: Given the perturbed state-space model (2), how can we update a nominal stabilizing SOF controller F such that the closed-loop system remains stable?

III. A Novel Update of a Nominal Stabilizing SOF Controller

This section consists of twofold: *(i)* motivation and *(ii) main idea*. First, we present what motivates us to propose a novel update of a nominal stabilizing SOF controller. Second, we detail the main idea behind the proposed updated stabilizing SOF controller.

A. Motivation

In order to improve the stability robustness of the perturbed state-space (2), let us consider the updated stabilizing SOF controller, as $F + G$, with the following state-space model:

$$\dot{x}(t) = (A + \Delta + B(F + G)C)x(t). \tag{3}$$

For instance, for the special case of the typical approach, $G^{\text{typical}} = F^{\text{typical}} - F$ holds.

Defining the notion of *minimum destabilizing real perturbation* (MDRP) of a given stable matrix $\mathcal{A} \in \mathbb{R}^{n\times n}$, namely $\beta_{\mathbb{R}}(\mathcal{A})$, as follows ((3.2) in [18]):

$$\beta_{\mathbb{R}}(\mathcal{A}) := \min\{\|\mathcal{X}\|_F : \alpha(\mathcal{A}+\mathcal{X}) = 0, \mathcal{X} \in \mathbb{R}^{n\times n}\},$$

and choosing $\mathcal{A} = A + BFC$ and $\mathcal{X} = BGC + \Delta$ based on the updated perturbed state-space model (3), we see that if

$$\|BGC + \Delta\|_F < \beta_{\mathbb{R}}(A + BFC), \tag{4}$$

holds, then $A + \Delta + B(F + G)C$ is stable, i.e., $F + G$ is an updated stabilizing SOF controller for $A + \Delta$. Inequality (4) motivates us to search for an efficient update $F + G$ via minimizing the $\|BGC + \Delta\|_F$.

In the sequel, we present the lower and upper bounds on MDRP of $A + BFC$ followed by a brief description of its exact value computation.

1) Lower bound: Considering the fact that $\alpha(X)$ is a continuous function with respect to X, we have by definition

$$\begin{aligned}&\forall\epsilon > 0, \exists\delta(\epsilon) > 0, \text{ s.t. if } \|\mathcal{X}\|_F < \delta(\epsilon) \text{ holds, then}\\ &\alpha(\mathcal{A}) - \epsilon < \alpha(\mathcal{A}+\mathcal{X}) < \alpha(\mathcal{A}) + \epsilon \text{ holds,}\end{aligned}$$

Then, choosing $\mathcal{A} = A+BFC$ and $\mathcal{X} = BGC+\Delta$, we realize that for any ϵ satisfying $\epsilon < -\alpha(A + BFC)$, if $\|BGC + \Delta\|_F < \delta(\epsilon)$ holds, then $A+\Delta+B(F+G)C$ is stable. That suggests the following lower bound on MDRP of $A + BFC$:

$$0 < \delta_{\text{sup}} \le \beta_{\mathbb{R}}(A + BFC), \tag{5a}$$
$$\delta_{\text{sup}} := \sup\{\delta(\epsilon) : \epsilon \in]0, -\alpha(A + BFC)[\}, \tag{5b}$$

2) Upper bound: On one hand, since $\alpha(\mathcal{A}+\mathcal{X}) = 0$ holds for the choice of $\mathcal{X} = -\alpha(\mathcal{A})I_n$, then choosing $\mathcal{A} = A + BFC$ and $\mathcal{X} = -\alpha(A+BFC)I_n$, we get the following upper bound on MDRP of $A + BFC$ [18]:

$$\beta_{\mathbb{R}}(A + BFC) \le -\sqrt{n}\alpha(A + BFC). \tag{6}$$

On the other hand, given $\mathcal{A} = U_{\mathcal{A}}\Sigma_{\mathcal{A}}V_{\mathcal{A}}^T$ as the singular value decomposition (SVD) of $\mathcal{A}$ and choosing $\mathcal{X} = -\sigma_{\mathcal{A}}^{\min}u_{\mathcal{A}}^{\min}v_{\mathcal{A}}^{\min\,T}$ (superscript $\min$ denotes the corresponding minimum singular value and vectors), it can be verified that $\alpha(\mathcal{A} + \mathcal{X}) = 0$ holds. Then, choosing $\mathcal{A} = A + BFC$ and according to (6), we get the following upper bound on MDRP of $A + BFC$ [18]:

$$\beta_{\mathbb{R}}(A + BFC) \le \beta_{\mathbb{R}}^u, \tag{7a}$$
$$\beta_{\mathbb{R}}^u = \min\{\sigma^{\min}(A + BFC), -\sqrt{n}\alpha(A + BFC)\}. \tag{7b}$$

For the special case of a diagonalizable $A + BFC$ with the eigendecomposition $A + BFC = V\Lambda V^{-1}$, since $\sigma^{\min}(A + BFC) = -\alpha(A + BFC)$ holds, (7) reduces to

$$\beta_{\mathbb{R}}(A + BFC) \le -\alpha(A + BFC), \tag{8}$$

which is a tighter bound compared to the upper bound in (6). Specifically, for the case of symmetric $A + BFC$, according to Corollary 3.5. in [22], the equality in (8) holds.

3) Exact value: Unfortunately, computing the exact value of $\beta_{\mathbb{R}}(A+BFC)$ is not theoretically possible [18]. Also, there is no systematic tractable way to compute the exact value of the lower bound δ_{sup} in (5) due to the fact that we only know about the existence of $\delta(\epsilon)$ and nothing more. However, taking advantage of the upper bounds on $\beta_{\mathbb{R}}(A + BFC)$ (derived in (7) and (8)), we may utilize heuristics to obtain an appropriate approximate value of $\beta_{\mathbb{R}}(A + BFC)$ in a reasonable computational time. It is remarkable that if the equality in (7) becomes active (i.e., the case of a tight upper bound), then the proposed updated stabilizing SOF controller in this paper becomes efficient as it only requires the value of $\beta_{\mathbb{R}}^u$ which can efficiently be computed (e.g., the case of a symmetric $A + BFC$ for which $\beta_{\mathbb{R}}(A + BFC) = -\alpha(A + BFC)$ holds). For the special case of structured perturbation, i.e., $\Delta = BMC$ for a matrix $M \in \mathbb{R}^{m\times p}$, one may compute MDRP via (frequency domain)-based algorithms detailed by [23].

B. Main idea

Since (4) provides a sufficient condition on the stability of $A + \Delta + B(F + G)C$, our main idea to propose an efficient updated stabilizing SOF controller $F + G$ is to compute G via minimizing $\|BGC + \Delta\|_F^2$ and verifying that under which conditions, the minimized value of $\|BGC + \Delta\|_F^2$ would be less than $\beta_{\mathbb{R}}(A + BFC)^2$. It is noteworthy that if the most optimistic scenario occurs, (i.e., the scenario in which for a known Δ, equation $\|BGC + \Delta\|_F = 0$ has a solution G), then one can completely cancel out the effect of the hitting perturbation Δ and retrieve the primary unperturbed $A+BFC$ as detailed later on.

With that in mind and to find a reasonable answer to the question stated in Section II (*Q1*), we consider the following optimization problem:

$$\min_{G\in\mathbb{R}^{m\times p}} \|BGC + \Delta\|_F^2. \tag{9}$$

By vectorizing $BGC + \Delta$, defining $g := \mathbf{vec}(G), \delta := \mathbf{vec}(\Delta), H := C^T \otimes B$, and noting that $\mathbf{vec}(\mathcal{XYZ}) = (\mathcal{Z}^T \otimes \mathcal{X})\mathbf{vec}(\mathcal{Y})$ holds for any triplet $(\mathcal{X}, \mathcal{Y}, \mathcal{Z})$ with consistent dimensions and $\|\mathbf{vec}(X)\| = \|X\|_F$ holds for any X, optimization problem (9) can equivalently be cast as the following least-squares problem [24]:

$$\min_{g\in\mathbb{R}^{mp}} \|Hg + \delta\|^2. \tag{10}$$

Assuming that B and C are respectively full-column rank and full-row rank and noting that identity $(C^T\otimes B)^+ = C^{T+}\otimes B^+$ holds, optimization problem (10) can analytically be solved as

$$g_\delta^* = -(C^{T+} \otimes B^+)\delta, \tag{11}$$

and the analytic optimal solution of (9) can subsequently be presented as follows:

$$G_\Delta^* = \mathbf{vec}^{-1}(g_\delta^*) = -B^+\Delta(C^{T+})^T, \tag{12}$$

for which the computation complexity is $\mathcal{O}(n^2\min\{m, p\})$ while the computation complexity of (11) is $\mathcal{O}(n^2m^2p^2)$.

Substituting g_δ^* of (11) in (10), the optimal value of the objective function in (10), namely $J^*(\delta)$, becomes

$$J^*(\delta) := \|Hg_\delta^* + \delta\|^2 = \|(I_{n^2} - HH^+)\delta\|^2. \quad (13)$$

Defining $P := I_{n^2} - HH^+$ and noting that $P^TP = P$ holds (since $H^+H = I_{mp}$ holds), (13) reduces to

$$J^*(\delta) = \delta^T P \delta. \quad (14)$$

For the sake of preciseness, with a bit of abuse of notation, we simply define $J^*(\Delta) := J^*(\mathbf{vec}(\Delta)) = J^*(\delta)$.

IV. Main Results

This section consists of the main results of the paper. The main results are twofold: *(i)* In Section IV-A, given a known norm-bounded perturbation Δ with $0 < \|\Delta\|_F \leq \rho$, we investigate the dependency of $J^*(\Delta)$ on Δ via inspecting the linear algebraic properties of P in (14). Proposition 1 analytically parameterizes the norm-bounded perturbation and proposes a closed-form formula for $J^*(\Delta)$. Proposition 2 elaborates on deriving sufficient conditions for the stability of the proposed updated stabilizing SOF controllers while analytically characterizing the guaranteed stability regions. Furthermore, we define a geometric metric to quantify the stability robustness of the proposed updated stabilizing SOF controllers, *(ii)* in Section IV-B, given an unknown norm-bounded perturbation Δ with a known upper bound ρ on its Frobenius norm, we derive sufficient conditions on the stability of the proposed updated stabilizing SOF controllers in Proposition 3. Proposition 4 mathematically characterizes the guaranteed stability regions for which the proposed updated SOF controllers are stabilizing. Similarly, we define a geometric metric to quantify the stability quality of the proposed updated stabilizing SOF controllers. Also, built upon a notion of *non-fragility* utilized in the literature of robust non-fragile PID controller designs [25]–[28], we propose non-fragility-based robust updated stabilizing SOF controllers. In the sequel, to save space, whenever needed, we refer to $\beta_{\mathbb{R}}(A + BFC)$ as β.

A. Known norm-bounded perturbation

In the following lemma, we present an SVD-based parameterization of P in (14) that facilitates parameterizing the norm-bounded perturbation Δ and subsequently proposing a closed-form expression for $J^*(\Delta)$.

Lemma 1. *Suppose that $H = U_H\Sigma_H V_H^T$ is the SVD of H. Then, P in (14) can be parameterized as follows:*

$$P = U_H \begin{bmatrix} 0 & 0 \\ 0 & I_{n^2-mp} \end{bmatrix} U_H^T, \quad (15)$$

where $U_H = (V_C \otimes U_B)U_\Omega$ holds provided that $B = U_B\Sigma_B V_B^T$, $C = U_C\Sigma_C V_C^T$, and $\Omega := \Sigma_C^T \otimes \Sigma_B = U_\Omega\Sigma_\Omega V_\Omega^T$ denote the SVDs of B, C, and Ω, respectively.

Proof: See Appendix A. ∎

1) Norm-bounded perturbation analytic parameterization: Built upon Lemma 1, we present the following proposition that analytically parameterizes the norm-bounded perturbation Δ while proposing a closed-form expression for $J^*(\Delta)$.

Proposition 1. *Given the norm-bounded perturbation Δ with $\|\Delta\|_F = r$ and $r \in]0, \rho]$, and considering $r = \rho\sin(\frac{\pi\tau}{2})$ with $\tau \in]0, 1]$, the norm-bounded perturbation Δ can be parameterized as follows:*

$$\Delta = \rho\sin\left(\frac{\pi\tau}{2}\right) U_B \mathbf{vec}^{-1}\left(U_\Omega \begin{bmatrix} \phi_c \cos(\frac{\pi\theta}{2}) \\ \phi_s \sin(\frac{\pi\theta}{2}) \end{bmatrix}\right) V_C^T, \quad (16)$$

where $\phi_c \in \mathbb{R}^{mp}$ with $\|\phi_c\| = 1$, $\phi_s \in \mathbb{R}^{n^2-mp}$ with $\|\phi_s\| = 1$, and $\theta \in [0, 1]$, and we can compute $J^*(\Delta)$ in (14) as follows:

$$J^*(\Delta) = \left(\rho\sin\left(\frac{\pi\tau}{2}\right)\sin\left(\frac{\pi\theta}{2}\right)\right)^2. \quad (17)$$

Proof: See Appendix B. ∎

The following corollary provides an alternative formula to compute G_Δ^* in (12).

Corollary 1. *Considering the following identities:*

$$(U_H, \Sigma_H, V_H) = ((V_C \otimes U_B)U_\Omega, \Sigma_\Omega, (U_C \otimes V_B)V_\Omega),$$
$$B = U_B\Sigma_B V_B^T, C = U_C\Sigma_C V_C^T, \Sigma_C^T \otimes \Sigma_B = U_\Omega\Sigma_\Omega V_\Omega^T,$$

(12) can alternatively be computed as follows:

$$G_\Delta^* = -\mathbf{vec}^{-1}(V_H \begin{bmatrix} (\begin{bmatrix} I_{mp} & 0 \end{bmatrix} \Sigma_H)^{-1} & 0 \end{bmatrix} U_H^T \mathbf{vec}(\Delta)).$$

Fig. 1 depicts the dependency of $\frac{J^*(\Delta)}{\rho^2}$ on τ and θ. As expected, since functions $\sin(\frac{\pi\tau}{2})$ and $\sin(\frac{\pi\theta}{2})$ have monotonic behaviors versus τ (for $\tau \in]0, 1]$) and θ (for $\theta \in [0, 1]$), respectively, the smaller τ and/or θ, the smaller $\frac{J^*(\Delta)}{\rho^2}$ we get. Note that the smaller value of $\frac{J^*(\Delta)}{\rho^2}$ is equivalent to the higher chance of satisfaction of the sufficient stability condition (4). In other words, its intuitive interpretation is that handling a less severe perturbation via an updated stabilizing SOF controller $F + G_\Delta^*$ with G_Δ^* in (12) is easier.

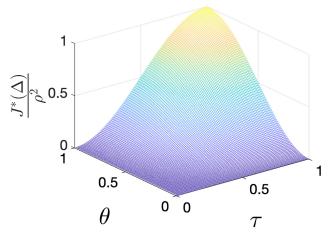

Figure 1. The dependency of $\frac{J^*(\Delta)}{\rho^2}$ on τ and θ.

2) The guaranteed stability region analytic characterization: We state the following proposition that derives sufficient conditions on the stability of the proposed updated stabilizing SOF controllers while analytically characterizing the guaranteed stability regions.

Proposition 2. *Given the norm-bounded perturbation Δ parameterized by (16), $F + G_\Delta^*$ with G_Δ^* in (12) is an updated stabilizing SOF controller,*

i . if $\rho < \beta_{\mathbb{R}}(A+BFC)$ holds.

ii . else if $\rho \geq \beta_{\mathbb{R}}(A+BFC)$ and $(\tau_\Delta, \theta_\Delta) \in S_\kappa$ hold where the guaranteed stability region S_κ is defined as:

$$S_\kappa := \check{S} \cup \tilde{S}, \tag{18a}$$

$$\check{S} := \{(\tau,\theta) : \tau \in]0,\kappa[, \theta \in [0,1]\}, \tag{18b}$$

$$\kappa := \frac{2}{\pi}\arcsin\Big(\frac{\beta_{\mathbb{R}}(A+BFC)}{\rho}\Big), \tag{18c}$$

$$\tilde{S} := \{(\tau,\theta) : \tau \in [\kappa,1], \theta \in [0,\zeta_{\tau,\kappa}[\}, \tag{18d}$$

$$\zeta_{\tau,\kappa} := \frac{2}{\pi}\arcsin\Big(\frac{\sin(\frac{\pi\kappa}{2})}{\sin(\frac{\pi\tau}{2})}\Big). \tag{18e}$$

Moreover, the following geometric metric provides a percentage-based lower bound on the stability of the updated perturbed state-space (3):

$$\xi_\kappa\ (\%) := 100 \times \Big(\kappa + \int_\kappa^1 \zeta_{\tau,\kappa} d\tau\Big), \tag{19}$$

and ξ_κ is an increasing function of κ (equivalently ξ_ρ is a decreasing function of ρ for a fixed $\beta_{\mathbb{R}}(A+BFC)$ and an increasing function of $\beta_{\mathbb{R}}(A+BFC)$ for a fixed ρ).

Proof: See Appendix C. ■

For the case of $\rho < \beta_{\mathbb{R}}(A+BFC)$, the guaranteed stability region would be $]0,1] \times [0,1] = S_\kappa|_{\kappa=1} \cup \{(1,1)\}$, i.e., the unit square in the non-negative quadrant of (τ,θ). For the sake of notation simplicity, we define $\mathbb{S} =]0,1] \times [0,1]$ and utilize the unified notation of S to refer to both guaranteed stability regions S_κ and $\mathbb{S}$. The following corollary thoroughly sheds light on the dependency and limiting behaviors of ξ_ρ and ξ_β on ρ and β, respectively.

Corollary 2. *For the case of $\rho \geq \beta_{\mathbb{R}}(A+BFC)$, considering the following expression for ξ_ρ:*

$$\xi_\rho = \frac{2}{\pi}\arcsin\Big(\frac{\beta}{\rho}\Big) + \frac{2}{\pi}\int_{\frac{2}{\pi}\arcsin\left(\frac{\beta}{\rho}\right)}^1 \arcsin\Big(\frac{\beta}{\rho\sin(\frac{\pi\tau}{2})}\Big)d\tau,$$

we compute the derivative of ξ_ρ with respect to ρ as follows:

$$\frac{d\xi_\rho}{d\rho} = -\frac{2}{\pi\rho}\int_{\frac{2}{\pi}\arcsin\left(\frac{\beta}{\rho}\right)}^1 \frac{\beta}{\rho\sqrt{\sin(\frac{\pi\tau}{2})^2 - (\frac{\beta}{\rho})^2}}d\tau. \tag{20}$$

Moreover, as ρ tends to β and ∞ in (20), we get

$$\lim_{\rho\to\beta^+}\frac{d\xi_\rho}{d\rho} = -\frac{2}{\pi\beta},\ \lim_{\rho\to\infty}\frac{d\xi_\rho}{d\rho} = 0,\ \lim_{\rho\to\beta^+}\xi_\rho = 1,\ \lim_{\rho\to\infty}\xi_\rho = 0.$$

Similarly, considering the following expression for ξ_β:

$$\xi_\beta = \frac{2}{\pi}\arcsin\Big(\frac{\beta}{\rho}\Big) + \frac{2}{\pi}\int_{\frac{2}{\pi}\arcsin\left(\frac{\beta}{\rho}\right)}^1 \arcsin\Big(\frac{\beta}{\rho\sin(\frac{\pi\tau}{2})}\Big)d\tau,$$

we compute the derivative of ξ_β with respect to β as follows:

$$\frac{d\xi_\beta}{d\beta} = \frac{2}{\pi\rho}\int_{\frac{2}{\pi}\arcsin\left(\frac{\beta}{\rho}\right)}^1 \frac{1}{\sqrt{\sin(\frac{\pi\tau}{2})^2 - (\frac{\beta}{\rho})^2}}d\tau. \tag{21}$$

Moreover, by tending β to 0 and ρ in (21), we get

$$\lim_{\beta\to0^+}\frac{d\xi_\beta}{d\beta} = \infty,\ \lim_{\beta\to\rho^-}\frac{d\xi_\beta}{d\beta} = \frac{2}{\pi\rho},\ \lim_{\beta\to0^+}\xi_\beta = 0,$$

$$\lim_{\beta\to\rho^-}\xi_\beta = 1.$$

Fig. 2 visualizes the guaranteed stability region S_κ for $\kappa = \frac{1}{3}$ and the percentage-based lower bounds on the stability of the updated perturbed state-space (3) versus κ, ρ, and β. As expected, the empirical observations of Fig. 2 are consistent with the theoretical results of Proposition 2 and Corollary 2. Precisely, as κ decreases, e.g., for an increased perturbation upper bound ρ or a decreased MDRP β, the percentage-based lower bound on the stability of the updated perturbed state-space (3) ξ (%) degrades which is expected. As Fig. 2 (Top-Left) depicts, for the sufficiently large values of τ and/or θ, i.e., more severe perturbations, (τ,θ) lies outside the S_κ and there is no stability guarantee for the proposed updated SOF controller which is aligned with the expectations around the negative impacts of perturbations on the stability.

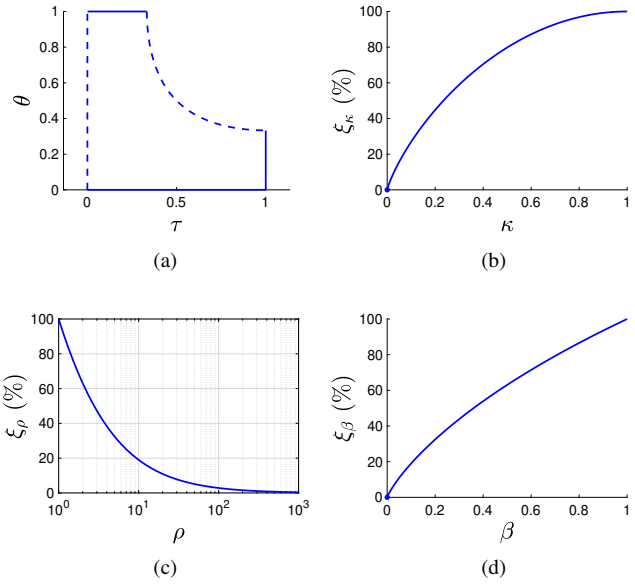

Figure 2. (a) The guaranteed stability region S_κ for $\kappa = \frac{1}{3}$, (b) the percentage-based lower bound on the stability of the updated perturbed state-space (3) ξ_κ (%) versus κ, (c) the percentage-based lower bound on the stability of the updated perturbed state-space (3) ξ_ρ (%) versus ρ for $\beta = 1$, and (d) the percentage-based lower bound on the stability of the updated perturbed state-space (3) ξ_β (%) versus β for $\rho = 1$.

B. Unknown norm-bounded perturbation

Given an unknown norm-bounded perturbation Δ with $0 < \|\Delta\|_F \leq \rho$, let us denote a known norm-bounded perturbation with an upper bound ρ on its Frobenius norm as $\hat{\Delta}$. We refer to $\hat{\Delta}$ as an *estimate* of unknown Δ. Also, whenever needed, for ease of representation, we will simply denote $\tau_{\hat{\Delta}}$ and $\theta_{\hat{\Delta}}$ with $\hat{\tau}$ and $\hat{\theta}$, respectively. Moreover, we represent the guaranteed stability regions associated with $\hat{\Delta}$ by $\hat{S}_\kappa$, $\hat{\mathbb{S}}$, and $\hat{S}$ (the unified notation for both $\hat{S}_\kappa$ and $\hat{\mathbb{S}}$). In the following proposition, we derive sufficient stability conditions under which the proposed updated SOF controllers are stabilizing.

Proposition 3. *Given an unknown norm-bounded perturbation Δ and its estimate $\hat{\Delta}$ both with an upper bound ρ on their*

Frobenius norms, $F+G^*_{\hat{\Delta}}$ with $G^*_{\hat{\Delta}}$ in (12) is an updated stabilizing SOF controller,

i . if $\rho<\beta_{\mathbb{R}}(A+BFC)$ and

$$\|\Delta-\hat{\Delta}\|_F<\upsilon, \tag{22a}$$

$$\upsilon:=\beta_{\mathbb{R}}(A+BFC)-\rho\sin\left(\frac{\pi\tau_{\hat{\Delta}}}{2}\right)\sin\left(\frac{\pi\theta_{\hat{\Delta}}}{2}\right), \tag{22b}$$

hold.

ii . if $\rho\geq\beta_{\mathbb{R}}(A+BFC)$, (22), and $(\tau_{\hat{\Delta}},\theta_{\hat{\Delta}})\in\hat{S}_\kappa$ hold.

Proof: See Appendix D. ∎

The following lemma enables us to have a more thorough quantitative understanding of the estimation inaccuracy and its dependency on various factors.

Lemma 2. *Given the Δ and $\hat{\Delta}$ as in Proposition 3, the following identity holds:*

$$\|\Delta-\hat{\Delta}\|_F=\rho\sqrt{s_\tau^2+s_{\hat{\tau}}^2-2s_\tau s_{\hat{\tau}}c_{2\eta}}, \tag{23a}$$

$$s_\tau:=\sin\left(\frac{\pi\tau_\Delta}{2}\right),s_{\hat{\tau}}:=\sin\left(\frac{\pi\tau_{\hat{\Delta}}}{2}\right), \tag{23b}$$

$$c_{2\eta}:=\cos(\pi\eta),\eta:=\frac{1}{\pi}\arccos(\psi^T\hat{\psi}), \tag{23c}$$

$$\psi:=\psi_\Delta,\hat{\psi}:=\psi_{\hat{\Delta}}. \tag{23d}$$

Proof: See Appendix E. ∎

Note that $\pi\eta$ denotes the phase difference between ψ and $\hat{\psi}$.

1) The guaranteed stability region mathematical characterization: Built upon Proposition 3 and Lemma 2, we present the following proposition that lists all the possible parametric scenarios for mathematically characterizing the guaranteed stability regions.

Proposition 4. *Given the Δ and $\hat{\Delta}$ as in Proposition 3 and defining*

$$s_{\hat{\theta}}:=\sin\left(\frac{\pi\theta_{\hat{\Delta}}}{2}\right),\iota:=\frac{\beta_{\mathbb{R}}(A+BFC)}{\rho s_{\hat{\tau}}}-s_{\hat{\theta}}=\frac{\upsilon}{\rho s_{\hat{\tau}}},$$

$$\bar{\eta}:=\frac{1}{\pi}\arcsin(\iota),\text{for }0<\iota\leq 1,\ \hat{b}:=\frac{s_{\hat{\tau}}}{2}(1-\iota^2)+\frac{1}{2s_{\hat{\tau}}},$$

$$\underline{\eta}:=\frac{1}{\pi}\arccos(\hat{b}),\text{for }|\hat{b}|\leq 1,\ s_{2\eta}:=\sin(\pi\eta),$$

$$b_l(\eta):=s_{\hat{\tau}}\left(c_{2\eta}-\sqrt{\iota^2-s_{2\eta}^2}\right),$$

$$\varphi_l(\eta):=\frac{2}{\pi}\arcsin(b_l(\eta)),\text{for }0\leq b_l(\eta)<1,$$

$$b_u(\eta):=s_{\hat{\tau}}\left(c_{2\eta}+\sqrt{\iota^2-s_{2\eta}^2}\right),$$

$$\varphi_u(\eta):=\frac{2}{\pi}\arcsin(b_u(\eta)),\text{for }0<b_u(\eta)\leq 1,$$

if $(\eta_\Delta,\tau_\Delta)\in\mathcal{S}$ holds, then $F+G^*_{\hat{\Delta}}$ with $G^*_{\hat{\Delta}}$ in (12) is an updated stabilizing SOF controller where the guaranteed stability region $\mathcal{S}$ in 2-dimensional parametric space of (η,τ) can be characterized via the following itemized approach:

i . if $0<\iota\leq 1$ and $\hat{b}\leq 1$ hold, then $\mathcal{S}$ is defined as

$$\mathcal{S}:=\check{\mathcal{S}}\cup\tilde{\mathcal{S}}, \tag{24a}$$

$$\check{\mathcal{S}}:=\{(\eta,\tau):\eta\in[0,\underline{\eta}[,\tau\in]\varphi_l(\eta),1]\}, \tag{24b}$$

$$\tilde{\mathcal{S}}:=\{(\eta,\tau):\eta\in[\underline{\eta},\bar{\eta}[,\tau\in]\varphi_l(\eta),\varphi_u(\eta)[\}, \tag{24c}$$

ii . if $0<\iota\leq 1$ and $\hat{b}>1$ hold, then $\mathcal{S}$ is defined as

$$\mathcal{S}:=\{(\eta,\tau):\eta\in[0,\bar{\eta}[,\tau\in]\varphi_l(\eta),\varphi_u(\eta)[\}, \tag{25}$$

iii . if $\iota>1$ and $|\hat{b}|\leq 1$ hold, then $\mathcal{S}$ is defined as

$$\mathcal{S}:=\check{\mathcal{S}}\cup\tilde{\mathcal{S}}, \tag{26a}$$

$$\check{\mathcal{S}}:=\{(\eta,\tau):\eta\in[0,\underline{\eta}[,\tau\in]0,1]\}, \tag{26b}$$

$$\tilde{\mathcal{S}}:=\{(\eta,\tau):\eta\in[\underline{\eta},1],\tau\in]0,\varphi_u(\eta)[\}, \tag{26c}$$

iv . if $\iota>1$ and $\hat{b}>1$ hold, then $\mathcal{S}$ is defined as

$$\mathcal{S}:=\{(\eta,\tau):\eta\in[0,1],\tau\in]0,\varphi_u(\eta)[\}, \tag{27}$$

v . if $\iota>1$ and $\hat{b}<-1$ hold, then $\mathcal{S}$ is defined as

$$\mathcal{S}:=\{(\eta,\tau):\eta\in[0,1],\tau\in]0,1]\}, \tag{28}$$

Moreover, if $\rho<\beta_{\mathbb{R}}(A+BFC)$ holds, then $0<\iota$ automatically holds. Also, in the case of $\rho\geq\beta_{\mathbb{R}}(A+BFC)$, $0<\iota$ holds if and only if $(\tau_{\hat{\Delta}},\theta_{\hat{\Delta}})\in\hat{S}_\kappa$ holds.

Proof: See Appendix F. ∎

Utilizing the following equivalences:

$$\iota>0\iff s_{\hat{\tau}}s_{\hat{\theta}}\leq\frac{\beta}{\rho},\ \iota\leq 1\iff\frac{\beta}{\rho}\leq s_{\hat{\tau}}(s_{\hat{\theta}}+1),$$

$$\hat{b}\leq 1\iff\iota\geq\frac{1}{s_{\hat{\tau}}}-1\iff 1+s_{\hat{\tau}}(s_{\hat{\theta}}-1)\leq\frac{\beta}{\rho},$$

$$\hat{b}\geq -1\iff\iota\leq\frac{1}{s_{\hat{\tau}}}+1\iff\frac{\beta}{\rho}\leq 1+s_{\hat{\tau}}(s_{\hat{\theta}}+1),$$

the following corollary facilitates the itemized characterization proposed by Proposition 4.

Corollary 3. *The items presented by Proposition 4 can be simplified into the following items:*

i . if $1+s_{\hat{\tau}}(s_{\hat{\theta}}-1)\leq\frac{\beta}{\rho}\leq s_{\hat{\tau}}(s_{\hat{\theta}}+1)$ and $\frac{1}{3}\leq\tau_{\hat{\Delta}}\leq 1$ hold.

ii . 1) if $s_{\hat{\tau}}s_{\hat{\theta}}<\frac{\beta}{\rho}\leq s_{\hat{\tau}}(s_{\hat{\theta}}+1)$ and $0<\tau_{\hat{\Delta}}<\frac{1}{3}$ hold,
or
2) if $s_{\hat{\tau}}s_{\hat{\theta}}<\frac{\beta}{\rho}<1+s_{\hat{\tau}}(s_{\hat{\theta}}-1)$ and $\frac{1}{3}\leq\tau_{\hat{\Delta}}<1$ hold.

iii . 1) if $1+s_{\hat{\tau}}(s_{\hat{\theta}}-1)\leq\frac{\beta}{\rho}\leq 1+s_{\hat{\tau}}(s_{\hat{\theta}}+1)$ and $0<\tau_{\hat{\Delta}}<\frac{1}{3}$ hold,
or
2) if $s_{\hat{\tau}}(s_{\hat{\theta}}+1)<\frac{\beta}{\rho}\leq 1+s_{\hat{\tau}}(s_{\hat{\theta}}+1)$ and $\frac{1}{3}\leq\tau_{\hat{\Delta}}\leq 1$ hold.

iv . if $s_{\hat{\tau}}(s_{\hat{\theta}}+1)<\frac{\beta}{\rho}<1+s_{\hat{\tau}}(s_{\hat{\theta}}-1)$ and $0<\tau_{\hat{\Delta}}<\frac{1}{3}$ hold.

v . if $1+s_{\hat{\tau}}(s_{\hat{\theta}}+1)<\frac{\beta}{\rho}$ holds.

Note that the upper bounds of $\frac{\beta}{\rho}$ in item *ii* in Corollary 3 and the lower bounds of $\frac{\beta}{\rho}$ in item *iii* in Corollary 3 can compactly be expressed as follows:

$$ii.\ s_{\hat{\tau}}s_{\hat{\theta}}+\min\{s_{\hat{\tau}},1-s_{\hat{\tau}}\},$$
$$iii.\ s_{\hat{\tau}}s_{\hat{\theta}}+\max\{s_{\hat{\tau}},1-s_{\hat{\tau}}\},$$

where highlights the appearance of the threshold $\tau_{\hat{\Delta}}=\frac{1}{3}$, i.e., $\|\hat{\Delta}\|_F=\frac{\rho}{2}$.

Fig. 3 illustrates the guaranteed stability region $\mathcal{S}$ in 2-dimensional parametric space of (η,τ) for various cases itemized by Corollary 3. It is remarkable that item *v* in Corollary

3 can only occur for the case of $\rho < \beta$ as $1 < 1 + s_{\hat{\tau}}(s_{\hat{\theta}} + 1)$ should be satisfied. Also, the non-trivial boundary points with $\eta = 0$ ($(0, \tau_l^0)$ and $(0, \tau_u^0)$) or $\eta = 1$ ($(0, \tau_u^1)$) can be computed via the following formulas:

$$\tau_l^0 = \frac{2}{\pi} \arcsin\left(s_{\hat{\tau}}(1 + s_{\hat{\theta}}) - \frac{\beta}{\rho}\right),$$
$$\tau_u^0 = \frac{2}{\pi} \arcsin\left(s_{\hat{\tau}}(1 - s_{\hat{\theta}}) + \frac{\beta}{\rho}\right),$$
$$\tau_u^1 = \frac{2}{\pi} \arcsin\left(s_{\hat{\tau}}(-1 - s_{\hat{\theta}}) + \frac{\beta}{\rho}\right).$$

It is noteworthy that the extreme cases $\eta = 0$ (no phase difference) and $\eta = 1$ (maximum phase difference) represent the special cases $\hat{\psi} = \psi$ and $\hat{\psi} = -\psi$, respectively.

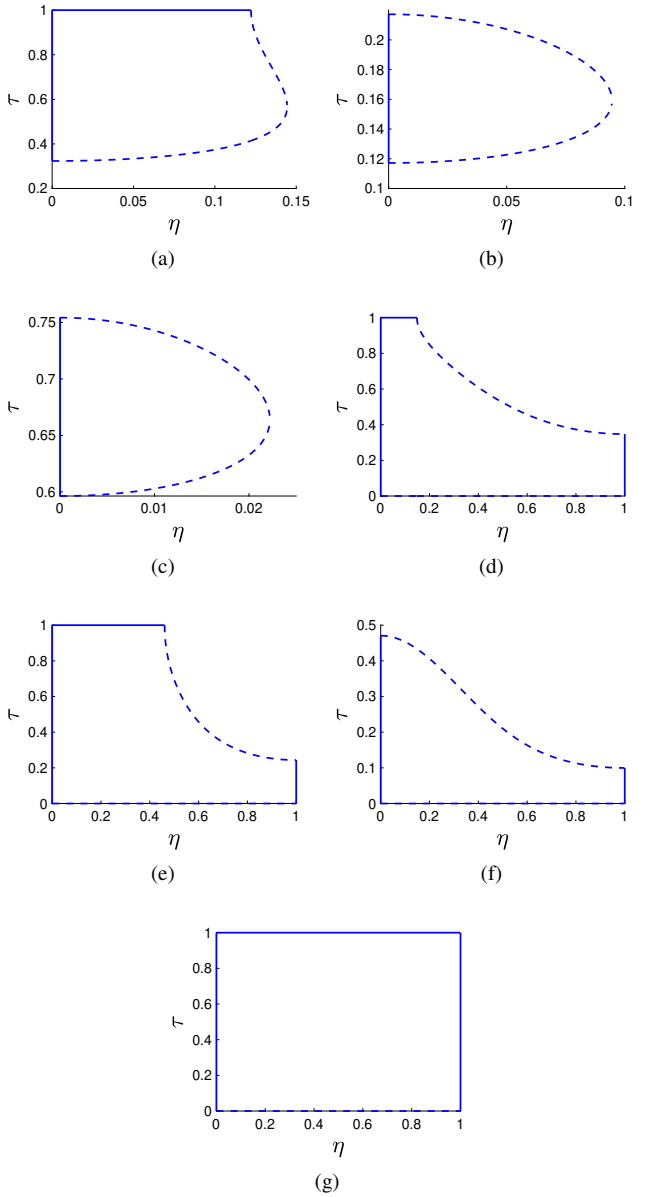

Figure 3. The guaranteed stability region $\mathcal{S}$ in 2-dimensional parametric space of (η, τ) for various cases itemized by Corollary 3 (a) *i*, (b) *ii-1*, (c) *ii-2*, (d) *iii-1*, (e) *iii-2*, (f) *iv*, and (g) *v*.

Similar to the case with known perturbation, we define a geometric metric to provide a percentage-based lower bound on the stability of the updated perturbed state-space (3). Given the guaranteed stability region $\mathcal{S}$ in 2-dimensional parametric space of (η, τ) (as presented by Proposition 4 and Corollary 3), we define the following geometric metric:

$$\Xi_{\tau_{\hat{\Delta}}, \theta_{\hat{\Delta}}; \frac{\beta}{\rho}, n}\ (\%) := 100 \times \frac{\mathcal{V}_{n^2}(\mathtt{D}(\mathcal{S}))}{\mathcal{V}_{n^2}(\mathtt{S}_\rho^{n^2})}. \tag{29}$$

where $\mathcal{V}_N(.)$, $\mathtt{S}_r^N$, and $\mathtt{D}(\mathcal{S})$ denotes the N-dimensional volume of an object, N-dimensional hypersphere of radius r centered at origin, and set of all δ with $\|\mathbf{vec}^{-1}(\delta)\|_F \leq \rho$ corresponding to $\mathcal{S}$.

In order to compute $\Xi_{\tau_{\hat{\Delta}}, \theta_{\hat{\Delta}}; \frac{\beta}{\rho}, n}\ (\%)$ (defined by (29)), we need to compute $\mathcal{V}_{n^2}(\mathtt{D}(\mathcal{S}))$ and $\mathcal{V}_{n^2}\left(\mathtt{S}_\rho^{n^2}\right)$. We compute both volumes via integral computation techniques similarly utilized by [29]. First, $\mathcal{V}_{n^2}\left(\mathtt{S}_\rho^{n^2}\right)$ can simply be computed as follows:

$$\mathcal{V}_{n^2}\left(\mathtt{S}_\rho^{n^2}\right) = \frac{\pi^{\frac{n^2}{2}} \rho^{n^2}}{\Gamma\left(\frac{n^2}{2} + 1\right)}. \tag{30}$$

Second, according to the spherical symmetry, $\mathcal{V}_{n^2}(\mathtt{D}(\mathcal{S}))$ can be computed as follows:

$$\mathcal{V}_{n^2}(\mathtt{D}(\mathcal{S})) = \int_{\pi\eta_u}^{\pi\eta_l} f_u(\varphi) - f_l(\varphi)\ d\varphi, \tag{31a}$$
$$f_u(\varphi) := \mathcal{V}_{n^2-1}\left(\mathtt{S}_{r_u(\varphi)\sin(\varphi)}^{n^2-1}\right) \frac{d(r_u(\varphi)\cos(\varphi))}{d\varphi}, \tag{31b}$$
$$f_l(\varphi) := \mathcal{V}_{n^2-1}\left(\mathtt{S}_{r_l(\varphi)\sin(\varphi)}^{n^2-1}\right) \frac{d(r_l(\varphi)\cos(\varphi))}{d\varphi}. \tag{31c}$$

where $\varphi := \pi\eta$, $r := \rho\sin(\frac{\pi\tau}{2})$, and $r_u(\varphi)/\eta_u$ and $r_l(\varphi)/\eta_l$ represent the upper and lower curves/bounds corresponding to $\mathcal{S}$, respectively. Note that the following identities:

$$\mathcal{V}_{n^2-1}\left(\mathtt{S}_{r_u(\varphi)\sin(\varphi)}^{n^2-1}\right) = \frac{\pi^{\frac{n^2-1}{2}} (r_u(\varphi)\sin(\varphi))^{n^2-1}}{\Gamma\left(\frac{n^2-1}{2} + 1\right)}, \tag{32a}$$
$$\mathcal{V}_{n^2-1}\left(\mathtt{S}_{r_l(\varphi)\sin(\varphi)}^{n^2-1}\right) = \frac{\pi^{\frac{n^2-1}{2}} (r_l(\varphi)\sin(\varphi))^{n^2-1}}{\Gamma\left(\frac{n^2-1}{2} + 1\right)}, \tag{32b}$$
$$\frac{d(r_u(\varphi)\cos(\varphi))}{d\varphi} = -r_u(\varphi)\sin(\varphi) + \frac{dr_u(\varphi)}{d\varphi}\cos(\varphi), \tag{32c}$$
$$\frac{d(r_l(\varphi)\cos(\varphi))}{d\varphi} = -r_l(\varphi)\sin(\varphi) + \frac{dr_l(\varphi)}{d\varphi}\cos(\varphi), \tag{32d}$$

hold. Then, utilizing (30), (31), and (32) enables us to compute $\Xi_{\tau_{\hat{\Delta}}, \theta_{\hat{\Delta}}; \frac{\beta}{\rho}, n}\ (\%)$.

Fig. 4 depicts the dependency of $\Xi_{\tau_{\hat{\Delta}}, \theta_{\hat{\Delta}}; \frac{\beta}{\rho}, n}\ (\%)$ on $\tau_{\hat{\Delta}}$ and $\theta_{\hat{\Delta}}$ for $\frac{\beta}{\rho} = \frac{1}{2}$ and $n = 4$. As observed, approaching the origin, the value of the geometric metric gets improved (a maximum value of $1.5259 \times 10^{-3}\%$), meaning that a larger amount of perturbations can be handled provided that they are less severe. Similarly, approaching the instability boundary, the value of the geometric metric gets degraded, that is, a smaller amount of perturbations can be handled provided that they are more severe. Then, there exists a fundamental trade-off between the potential severeness of perturbations and the successfully handled amount of perturbations.

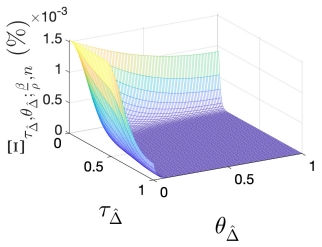

Figure 4. The dependency of $\Xi_{\tau_{\hat{\Delta}},\theta_{\hat{\Delta}};\frac{\beta}{\rho},n}$ (%) (defined by (29)) on $\tau_{\hat{\Delta}}$ and $\theta_{\hat{\Delta}}$ for $\frac{\beta}{\rho}=\frac{1}{2}$ and $n=4$.

2) Non-fragility-based robust update: Inspired by Propositions 1, 2, 3, and 4 and employing a notion of *non-fragility* (NF) utilized by [25]–[28], we propose a robust update for the case of dealing with an unknown norm-bounded perturbation Δ with a known upper bound ρ on its Frobenius norm, based on the following criterion:

C1: Choose the point deepest inside the guaranteed stability region $\hat{S}$ (i.e., farthest from the boundary) as a robust update. To choose the point deepest inside the guaranteed stability region $\hat{S}$, we utilize three well-known geometric notions: *(i)* Chebyshev center, *(ii)* centroid, and *(iii) weighted centroid*.

Chebyshev center: A robust update based on the Chebyshev center can be computed as follows:

$$G^*_{\hat{\Delta}_{\rm NF}} = -B^+\hat{\Delta}_{\rm NF}(C^{T+})^T, \tag{33a}$$

$$\hat{\Delta}_{\rm NF} = \rho\sin\left(\frac{\pi\hat{\tau}_{\rm NF}}{2}\right)\mathbf{vec}^{-1}\left(U_H\begin{bmatrix}\hat{\phi}_c\cos(\frac{\pi\hat{\theta}_{\rm NF}}{2})\\ \hat{\phi}_s\sin(\frac{\pi\hat{\theta}_{\rm NF}}{2})\end{bmatrix}\right), \tag{33b}$$

$$\hat{\tau}_{\rm NF} = \frac{4-2\sqrt{2}}{\pi}\arcsin\left(\sqrt{\frac{\beta}{\rho}}\right), \hat{\theta}_{\rm NF}=\hat{\tau}_{\rm NF}. \tag{33c}$$

Centroid: A robust update based on centroid can be computed as follows:

$$G^*_{\hat{\Delta}_{\rm NF}} = -B^+\hat{\Delta}_{\rm NF}(C^{T+})^T, \tag{34a}$$

$$\hat{\Delta}_{\rm NF} = \rho\sin\left(\frac{\pi\hat{\tau}_{\rm NF}}{2}\right)\mathbf{vec}^{-1}\left(U_H\begin{bmatrix}\hat{\phi}_c\cos(\frac{\pi\hat{\theta}_{\rm NF}}{2})\\ \hat{\phi}_s\sin(\frac{\pi\hat{\theta}_{\rm NF}}{2})\end{bmatrix}\right), \tag{34b}$$

$$\hat{\tau}_{\rm NF} = \frac{\int_{\hat{S}}\hat{\tau}d\hat{\theta}d\hat{\tau}}{\int_{\hat{S}}d\hat{\theta}d\hat{\tau}}, \hat{\theta}_{\rm NF} = \frac{\int_{\hat{S}}\hat{\theta}d\hat{\theta}d\hat{\tau}}{\int_{\hat{S}}d\hat{\theta}d\hat{\tau}}. \tag{34c}$$

wherein $\hat{\theta}_{\rm NF}=\hat{\tau}_{\rm NF}$ holds due to the symmetry of $\hat{S}$ with respect to $\hat{\theta}=\hat{\tau}$.
Specifically, for the case of $\rho<\beta_{\mathbb{R}}(A+BFC)$, both of the robust updates in (33) and (34) reduce to the following form:

$$G^*_{\hat{\Delta}_{\rm NF}} = -B^+\hat{\Delta}_{\rm NF}(C^{T+})^T, \tag{35a}$$

$$\hat{\Delta}_{\rm NF} = \frac{\rho}{2}\mathbf{vec}^{-1}\left(U_H\begin{bmatrix}\hat{\phi}_c\\ \hat{\phi}_s\end{bmatrix}\right). \tag{35b}$$

Note that in (35) $(\hat{\tau}_{\rm NF},\hat{\theta}_{\rm NF})=(\frac{1}{2},\frac{1}{2})$ holds as $\hat{S}=\hat{\mathbb{S}}$ holds.

Weighted centroid: A robust update based on a weighted centroid can be computed as follows:

$$G^*_{\hat{\Delta}_{\rm NF}} = -B^+\hat{\Delta}_{\rm NF}(C^{T+})^T, \tag{36a}$$

$$\hat{\Delta}_{\rm NF} = \rho\sin\left(\frac{\pi\hat{\tau}_{\rm NF}}{2}\right)\mathbf{vec}^{-1}\left(U_H\begin{bmatrix}\hat{\phi}_c\cos(\frac{\pi\hat{\theta}_{\rm NF}}{2})\\ \hat{\phi}_s\sin(\frac{\pi\hat{\theta}_{\rm NF}}{2})\end{bmatrix}\right), \tag{36b}$$

$$\hat{\tau}_{\rm NF} = \frac{\int_{\hat{S}}\Xi(\hat{\tau},\hat{\theta})\hat{\tau}d\hat{\theta}d\hat{\tau}}{\int_{\hat{S}}\Xi(\hat{\tau},\hat{\theta})d\hat{\theta}d\hat{\tau}}, \hat{\theta}_{\rm NF} = \frac{\int_{\hat{S}}\Xi(\hat{\tau},\hat{\theta})\hat{\theta}d\hat{\theta}d\hat{\tau}}{\int_{\hat{S}}\Xi(\hat{\tau},\hat{\theta})d\hat{\theta}d\hat{\tau}}. \tag{36c}$$

The following corollary highlights that since $G^*_{\hat{\Delta}_{\rm NF}}$ in (33), (34), and (36) all lie inside the guaranteed stability region $\hat{S}$, the corresponding $F+G^*_{\hat{\Delta}_{\rm NF}}$ is a robust updated stabilizing SOF controller.

Corollary 4. *Given an unknown norm-bounded perturbation Δ with an upper bound ρ on its Frobenius norm, then $F+G^*_{\hat{\Delta}_{\rm NF}}$ with $G^*_{\hat{\Delta}_{\rm NF}}$ in (33), (34), and (36) is a robust updated stabilizing SOF controller.*

We highlight that for an arbitrary choice of $(\hat{\tau},\hat{\theta})$, one can similarly compute the corresponding $G^*_{\hat{\Delta}}$ via

$$G^*_{\hat{\Delta}} = -B^+\hat{\Delta}(C^{T+})^T, \tag{37a}$$

$$\hat{\Delta} = \rho\sin\left(\frac{\pi\hat{\tau}}{2}\right)\mathbf{vec}^{-1}\left(U_H\begin{bmatrix}\hat{\phi}_c\cos(\frac{\pi\hat{\theta}}{2})\\ \hat{\phi}_s\sin(\frac{\pi\hat{\theta}}{2})\end{bmatrix}\right). \tag{37b}$$

Given (ρ,n), computing $(\beta_{\mathbb{R}}(A+BFC),\hat{\tau}_{\rm NF},\hat{\theta}_{\rm NF})$, and having access to sufficiently accurate estimates $(\hat{\phi}_c,\hat{\phi}_s)$ of (ϕ_c,ϕ_s), we can utilize (33), (34), and (36) to propose robust updated stabilizing SOF controllers.

V. Numerical Simulations

This section is naturally divided into two main parts: *(i)* known norm-bounded perturbation and *(ii)* unknown norm-bounded perturbation. To assess the effectiveness of the theoretical results, we employ two benchmarks of the SOF controller benchmarks collected by [30]. To design a nominal stabilizing SOF controller F, we utilize MATLAB built-in function `hinfstruct(.)` [31] that has been developed built upon [32] to synthesize structured $\mathcal{H}_\infty$ controllers.

As mentioned earlier in the paper, computing the exact value of MDRP β is theoretically impossible. However, we utilize the following optimization problem:

$$\max_{v\in\mathbb{R}^{n^2},\ \beta\in\mathbb{R}_{++}} \alpha\left(A+BFC+\beta\mathbf{vec}^{-1}\left(\frac{v}{\|v\|}\right)\right). \tag{38}$$

along with a specialized bisection method (fixing the value of β and solving for a $v\in\mathbb{R}^{n^2}$), to obtain a near-optimal value of β. We initialize β with $\beta^u_{\mathbb{R}}$ and at each step, we check if the maximum value, namely α^*, is non-negative or not. To solve the optimization problem, one could utilize MATLAB's built-in function `fminunc(.)`. We put an emphasis that the efficiency of the proposed updated stabilizing SOF controller mainly depends on the computational efficiency of MDRP β as the computation complexity of (12) is $\mathcal{O}(n^2\min\{m,p\})$.

A. Known norm-bounded perturbation

Let us consider a lateral axis model of an $L-1011$ aircraft in cruise flight conditions ($AC3$) [30]. We design the following nominal stabilizing SOF controller F via `hinfstruct(.)`:

$$F=\begin{bmatrix}0 & 0 & 0 & -0.5057\\ 0.7521 & 0 & -3.0713 & 1.1408\end{bmatrix}.$$

for which $\alpha(A+BFC+\Delta)=0.0483$ (i.e., a destabilizing Δ), $\beta=0.1931$, and $\beta^u_{\mathbb{R}}=0.3230$ hold.

Fig. 5 (Left) visualizes the stability regions for $AC3$ benchmark with $\frac{\beta}{\rho}=\frac{1}{2}$: the guaranteed (conservative) stability region based on Proposition 2 and the exact one based on $\alpha(A+BFC+\Delta+BG^*_\Delta C)<0$ with G^*_Δ in (12). As expected, the guaranteed (conservative) stability region is a subset of the exact one. For instance, the update G^*_Δ for $(\tau_\Delta,\theta_\Delta)=(0.45,0.45)$ is as follows:

$$G^*_\Delta=\begin{bmatrix}0.0745 & -0.2034 & 0.0214 & -0.0939\\ 0.0115 & -0.0302 & 0.0018 & -0.0169\end{bmatrix},$$

for which $\alpha(A+BFC+\Delta+BG^*_\Delta C)=-0.0637$ holds and the updated stabilizing SOF controller $F+G^*_\Delta$ is as follows:

$$F+G^*_\Delta=\begin{bmatrix}0.0745 & -0.2034 & 0.0214 & -0.5996\\ 0.7636 & -0.0302 & -3.0695 & 1.1239\end{bmatrix}.$$

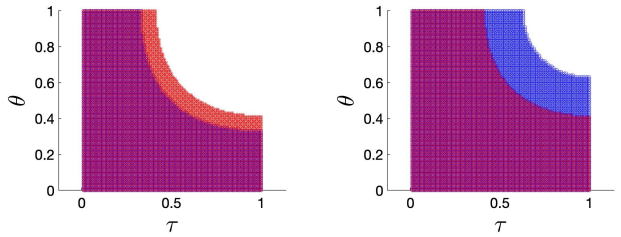

(a) (b)

Figure 5. The stability regions for $AC3$ benchmark with (a) $\rho=2\beta^{\text{accurate}}$ and $\beta=\beta^{\text{accurate}}$ and (b) $\rho=2\beta^{\text{accurate}}$ and $\beta=\beta^{\text{inaccurate}}$: the guaranteed (conservative) stability regions based on Proposition 2 (filled with blue circles) and the exact ones based on $\alpha(A+BFC+\Delta+BG^*_\Delta)<0$ with G^*_Δ in (12) (filled with red asterisks).

It is remarkable that the accurate computing of β plays a significant role in accurately identifying the stability regions. As Fig. 5 (Right) depicts, choosing ρ equal to 2×0.1931 (as chosen for Fig. 5 (Left)) and β equal to 0.3230 (an inaccurate value), leads to the misleading stability regions. First, the guaranteed (conservative) stability region has erroneously been enlarged. Second, the guaranteed (conservative) stability region has erroneously become the superset of the exact one.

B. Unknown norm-bounded perturbation

Let us consider the autopilot control problem for an air-to-air missile ($AC4$) [30]. The number of states for such a control problem is $n=4$. For $\frac{\beta}{\rho}=\frac{1}{2}$ and $n=4$, we get the following NF-based designs:

$$(\hat\tau^{\text{Cheb. center}}_{\text{NF}},\hat\theta^{\text{Cheb. center}}_{\text{NF}})=\left(\frac{2-\sqrt{2}}{2},\frac{2-\sqrt{2}}{2}\right),$$
$$(\hat\tau^{\text{Centroid}}_{\text{NF}},\hat\theta^{\text{Centroid}}_{\text{NF}})=(0.3787,0.3787),$$
$$(\hat\tau^{\text{W-centroid}}_{\text{NF}},\hat\theta^{\text{W-centroid}}_{\text{NF}})=(0.1603,0.2278),$$

where attain $\Xi^{\text{Cheb. center}}_{\frac{\beta}{\rho},\tau_{\hat\Delta},\theta_{\hat\Delta}}=5.0077\times10^{-7}\%$, $\Xi^{\text{Centroid}}_{\frac{\beta}{\rho},\tau_{\hat\Delta},\theta_{\hat\Delta}}=2.0450\times10^{-10}\%$, and $\Xi^{\text{W-centroid}}_{\frac{\beta}{\rho},\tau_{\hat\Delta},\theta_{\hat\Delta}}=7.0944\times10^{-5}\%$, respectively.

Fig. 6 visualizes the guaranteed stability region $\mathcal{S}$ in 2-dimensional parametric space of (η,τ) for various NF-based robust updates. As observed, the weighted centroid update attains the best average performance as it considers both being far from the boundary and obtaining a large guaranteed stability region (i.e., a large value of the geometric metric). Also, unlike the Chebyshev center update and the centroid update, for the case of weighted centroid update the identity $\hat\theta_{\text{NF}}=\hat\tau_{\text{NF}}$ does not necessarily hold as $\Xi(c_1,c_2)=\Xi(c_2,c_1)$ does not necessarily hold for $c_1\neq c_2$. Fig. 7 illustrates the weighted centroid updates for $\frac{\beta}{\rho}=\frac{1}{2}$ and various values of n. As Fig. 7 depicts, the higher the dimension n, the closer to the origin, the weighted centroid update we get. Tab. I reflects the corresponding values of the geometric metric $\Xi_{\tau_{\hat\Delta},\theta_{\hat\Delta};\frac{\beta}{\rho},n}$ (%) for the weighted centroid updates with $\frac{\beta}{\rho}=\frac{1}{2}$ and various values of n. As Tab. I shows, the higher the dimension n, the smaller geometric metric $\Xi_{\tau_{\hat\Delta},\theta_{\hat\Delta};\frac{\beta}{\rho},n}$ (%) we get.

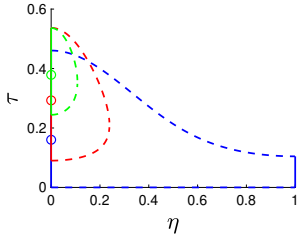

Figure 6. The guaranteed stability region $\mathcal{S}$ in 2-dimensional parametric space of (η,τ) for various NF-based robust updates (Chebyshev center in red, Centroid in green, and Weighted centroid in blue) for $\frac{\beta}{\rho}=\frac{1}{2}$ and $n=4$. Colored circles on the vertical axis represent the corresponding perturbations in the ideal case, i.e., $\hat\Delta_{\text{NF}}=\Delta$.

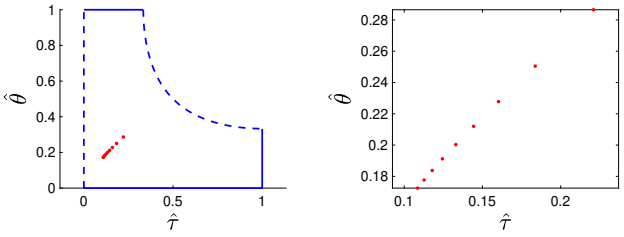

(a) (b)

Figure 7. The weighted centroid updates for $\frac{\beta}{\rho}=\frac{1}{2}$ and various values of n (a) inside $\hat S$ and (b) zoomed version.

Given an arbitrary point $(\eta^{\text{ap}},\tau^{\text{ap}})$ in 2-dimensional parametric space of (η,τ) and utilizing the itemized characterization proposed by Proposition 4, we visualize all the $(\hat\tau,\hat\theta)$'s belonging to $\hat S$ for which the guaranteed stability region $\mathcal{S}$ contains $(\eta^{\text{ap}},\tau^{\text{ap}})$. For instance, Fig. 8 depicts such a visualization for $(\eta^{\text{ap}},\tau^{\text{ap}})=(0.1,0.5)$ and $\frac{\beta}{\rho}=\frac{1}{2}$. Fig. 9 visualizes all the $G^*_{\hat\Delta}$-stabilizable points $(\eta^{\text{ap}},\tau^{\text{ap}})$ in 2-dimensional parametric space of (η,τ) for $\frac{\beta}{\rho}=\frac{1}{2}$. As expected, from Fig. 9, we realize that the perturbations with both high gain ($\propto\tau$) and high phase difference ($\propto\eta$) are not $G^*_{\hat\Delta}$–stabilizable.

Table I
THE CORRESPONDING VALUES OF THE GEOMETRIC METRIC $\Xi_{\tau_{\hat{\Delta}},\theta_{\hat{\Delta}};\frac{\beta}{\rho},n}$ (%) FOR THE WEIGHTED CENTROID UPDATES WITH $\frac{\beta}{\rho}=\frac{1}{2}$ AND VARIOUS VALUES OF n.

n	$(\hat{\tau}_{\rm NF}^{\rm W-centroid},\hat{\theta}_{\rm NF}^{\rm W-centroid})$	$\Xi_{\tau_{\hat{\Delta}},\theta_{\hat{\Delta}};\frac{\beta}{\rho},n}$ (%)
2	$(0.2210, 0.2865)$	$1.5360\times10^{0}\%$
3	$(0.1837, 0.2505)$	$2.1317\times10^{-2}\%$
4	$(0.1603, 0.2278)$	$7.0944\times10^{-5}\%$
5	$(0.1444, 0.2120)$	$5.5841\times10^{-8}\%$
6	$(0.1330, 0.2003)$	$1.0332\times10^{-11}\%$
7	$(0.1244, 0.1912)$	$4.4808\times10^{-16}\%$
8	$(0.1179, 0.1838)$	$4.5271\times10^{-21}\%$
9	$(0.1127, 0.1777)$	$1.0651\times10^{-26}\%$
10	$(0.1085, 0.1725)$	$5.8343\times10^{-33}\%$

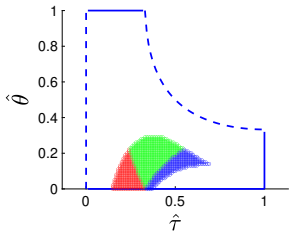

Figure 8. All the $(\hat{\tau},\hat{\theta})$'s belonging to $\hat{S}$ for which the guaranteed stability region $\mathcal{S}$ contains $(\eta^{\rm ap},\tau^{\rm ap})=(0.1,0.5)$ and $\frac{\beta}{\rho}=\frac{1}{2}$. Colored circles identify the corresponding items: item *iv* (filled with red circles), item *ii* (filled with green circles), and item *i* (filled with blue circles).

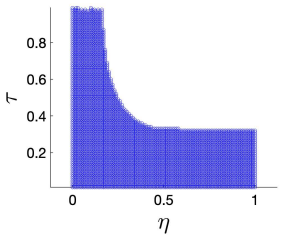

Figure 9. All the $G_{\hat{\Delta}}^{*}$-stabilizable points $(\eta^{\rm ap},\tau^{\rm ap})$ in 2-dimensional parametric space of (η,τ) for $\frac{\beta}{\rho}=\frac{1}{2}$.

Given a $G_{\hat{\Delta}}^{*}$-stabilizable point $(\eta^{\rm ap},\tau^{\rm ap})$ in 2-dimensional parametric space of (η,τ), we define the following geometric metric:

$$\mathcal{M}_{\eta,\theta;\frac{\beta}{\rho}}\ (\%):=100\times G_{\hat{\Delta}}^{*}-\text{stabilizing Region Area},\quad(39)$$

to quantify the $G_{\hat{\Delta}}^{*}$-stabilizability. Fig. 10 visualizes the $G_{\hat{\Delta}}^{*}$-stabilizability geometric metric $\mathcal{M}_{\eta,\theta;\frac{\beta}{\rho}}$ (%) for $\frac{\beta}{\rho}=\frac{1}{2}$. The larger $\mathcal{M}_{\eta,\theta;\frac{\beta}{\rho}}$ (%), the easier to stabilize a $G_{\hat{\Delta}}^{*}$-stabilizable point $(\eta^{\rm ap},\tau^{\rm ap})$ in 2-dimensional parametric space of (η,τ) we have. As Fig. 10 depicts, the largest value of $\mathcal{M}_{\eta,\theta;\frac{\beta}{\rho}}$ (%), i.e., 39.1386%, is attained by $(\eta^{\rm ap},\tau^{\rm ap})=(0,\frac{1}{3})$. A possible justification for such an observation can be the fact that $\eta^{\rm ap}=0$ corresponds to a zero phase difference and $\tau^{\rm ap}=\frac{1}{3}$ corresponds to $r=\frac{\rho}{2}=\frac{0+\rho}{2}$. Note that $\mathcal{M}_{\eta,\theta;\frac{\beta}{\rho}}$ (%) $=0\%$ in Fig. 10 represents the points $(\eta^{\rm ap},\tau^{\rm ap})$ in 2-dimensional parametric space of (η,τ) that are not $G_{\hat{\Delta}}^{*}$-stabilizable. Fig. 11 depicts the corresponding $G_{\hat{\Delta}}^{*}$-stabilizing region for $(\eta^{\rm ap},\tau^{\rm ap})=(0,\frac{1}{3})$.

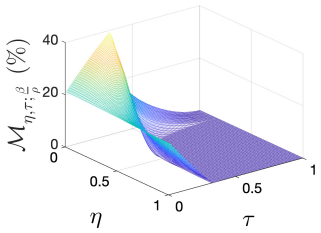

Figure 10. The $G_{\hat{\Delta}}^{*}$-stabilizability geometric metric $\mathcal{M}_{\eta,\theta;\frac{\beta}{\rho}}$ (%) for $\frac{\beta}{\rho}=\frac{1}{2}$.

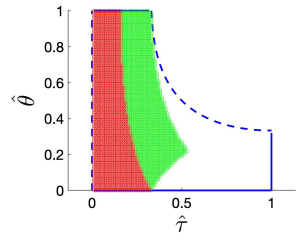

Figure 11. All the $(\hat{\tau},\hat{\theta})$'s belonging to $\hat{S}$ for which the guaranteed stability region $\mathcal{S}$ contains $(\eta^{\rm ap},\tau^{\rm ap})=(0,\frac{1}{3})$ and $\frac{\beta}{\rho}=\frac{1}{2}$. Colored circles identify the corresponding items: item *iv* (filled with red circles) and item *ii* (filled with green circles).

To empirically verify the relative performance of the weighted centroid update compared to the centroid update, the Chebyshev center update, and the update based on a point close to the origin $(\hat{\tau},\hat{\theta})=(0.01,0)$, we generate uniformly random samples of an unknown norm-bounded perturbation Δ with $0<\|\Delta\|_F\leq\rho$ [33] and check if $\|\Delta-\hat{\Delta}\|_F<\upsilon$ holds. To be more precise, we generate the uniformly random samples as follows:

$$\Delta=\mathbf{vec}^{-1}\left(r\frac{\vartheta}{\|\vartheta\|}\right),\ r\in\rho\times\mathcal{U}(0,1)^{\frac{1}{n^2}},\vartheta\in\mathcal{N}(0,I_{n^2}).$$

According to (23), considering

$$\psi=\begin{bmatrix}\phi_c\cos(\frac{\pi\theta}{2})\\ \phi_s\sin(\frac{\pi\theta}{2})\end{bmatrix},\hat{\psi}=\begin{bmatrix}\hat{\phi}_c\cos(\frac{\pi\hat{\theta}}{2})\\ \hat{\phi}_s\sin(\frac{\pi\hat{\theta}}{2}),\end{bmatrix}$$

and defining $(\gamma_c,\gamma_s):=(\phi_c^T\hat{\phi}_c,\phi_s^T\hat{\phi}_s)$, $c_\theta:=\cos(\frac{\pi\theta}{2})$, $s_\theta:=\sin(\frac{\pi\theta}{2})$, and $c_{\hat{\theta}}:=\cos(\frac{\pi\hat{\theta}}{2})$, we get

$$\eta=\frac{1}{\pi}\arccos(\psi^T\hat{\psi})=\frac{1}{\pi}\arccos(\gamma_c c_\theta c_{\hat{\theta}}+\gamma_s s_\theta s_{\hat{\theta}}).\quad(40)$$

It is noteworthy that $\gamma_c\in[-1,1]$ and $\gamma_s\in[-1,1]$ hold. For the ideal case of estimated $\hat{\Delta}$, i.e., $\hat{\Delta}=\Delta$, on the one hand, we have $\hat{\theta}=\theta$ and subsequently $(c_{\hat{\theta}},s_{\hat{\theta}})=(c_\theta,s_\theta)$. Also, we have $(\hat{\phi}_c,\hat{\phi}_s)=(\phi_c,\phi_s)$ and subsequently $(\gamma_c,\gamma_s)=(1,1)$. Consequently, according to (40), we observe that $\eta=0$ holds. On the other hand, for the ideal case of estimated $\hat{\Delta}$, $\hat{\tau}=\tau$ or equivalently $\hat{r}=r$ holds.

Since $U_H\psi=\frac{\vartheta}{\|\vartheta\|}$ and $U_H^TU_H=I_{n^2}$ hold, we have $\psi=U_H^T\frac{\vartheta}{\|\vartheta\|}$. Then, defining $\mu:=\begin{bmatrix}I_{mp} & 0\end{bmatrix}\psi$ and $\nu:=\begin{bmatrix}0 & I_{n^2-mp}\end{bmatrix}\psi$, we get

$$\phi_c=\frac{\mu}{\|\mu\|},\ \mu=\begin{bmatrix}I_{mp} & 0\end{bmatrix}U_H^T\frac{\vartheta}{\|\vartheta\|},\quad(41a)$$

$$\phi_s = \frac{\nu}{\|\nu\|},\ \nu = \begin{bmatrix} 0 & I_{n^2-mp} \end{bmatrix} U_H^T \frac{\vartheta}{\|\vartheta\|}, \tag{41b}$$

$$\theta = \frac{2}{\pi} \arcsin(\|\nu\|). \tag{41c}$$

Note that given ϑ, we can compute ϕ_c, ϕ_s, and θ via (41). In order to compute $G^*_{\hat{\Delta}}$ in (37), we need to choose $(\hat{\phi}_c, \hat{\phi}_s)$ given (γ_c, γ_s). The more accurate (γ_c, γ_s) (i.e., the larger values of γ_c and/or γ_s) and/or $(\hat{\tau}, \hat{\theta})$ (i.e., the smaller values of $\hat{\tau} - \tau$ and/or $\hat{\theta} - \theta$), the more accurate estimate $\hat{\Delta}$ we have. Given (γ_c, γ_s) and computing (ϕ_c, ϕ_s), we solve the following equations:

$$\phi_c^T \hat{\phi}_c - \gamma_c = 0, \phi_s^T \hat{\phi}_s - \gamma_s = 0, \tag{42}$$

for $(\hat{\phi}_c, \hat{\phi}_s)$ via the MATLAB built-in function `fsolve(.)`. We generate $N_\Delta = 10^6$ uniformly random samples inside the n^2-dimensional hypersphere of radius ρ centered at origin by the Cartesian product of $N_r = 10^4$ samples of r and $N_\vartheta = 10^2$ samples of ϑ.

Fig. 12 depicts the relative performance of the weighted centroid update compared to the centroid update, the Chebyshev center update, and the update based on a point close to the origin $(\hat{\tau}, \hat{\theta}) = (0.01, 0)$ for various choices of (γ_c, γ_s). As Fig. 12 shows, for the case of a more accurate estimate $\hat{\Delta}$ (i.e., the larger values of γ_c and/or γ_s), the weighted centroid update outperforms all the other updates. Interestingly, as the estimation quality degrades (i.e., the values of γ_c and/or γ_s decrease as visualized by the trend from Fig. 12 (Top-Left) to Fig. 12 (Bottom-Right)), a point close to the origin attains the best relative performance. Such an observation can be interpreted in this way that when we have no accurate information about the perturbation, the best strategy is choosing a point close to the origin (e.g., $(\hat{\tau}, \hat{\theta}) = (0.01, 0)$) as it attains the largest value of the geometric metric $\Xi_{\tau_{\hat{\Delta}}, \theta_{\hat{\Delta}}; \frac{\beta}{\rho}, n}$ (%). Also, as Fig. 12 (Top-Left) depicts, we observe that the Chebyshev center update outperforms the centroid update.

Fig. 13 depicts the corresponding plots for the case of checking $\|BG^*_{\hat{\Delta}} C + \Delta\|_F < \beta$ (the exact one) instead of $\|\Delta - \hat{\Delta}\|_F < \upsilon$ (the guaranteed (conservative) stability region). Similar observations/trends to the observations/trends depicted in Fig. 12 are also observed in Fig. 13. One difference is that fortunately, the relative performance of the NF-based robust updates in the exact scenario can be better than the guaranteed (conservative) scenario.

Fig. 14 visualizes the relative performance (both guaranteed (conservative) and exact scenarios) of the weighted centroid update compared to the centroid update, the Chebyshev center update, and the update based on a randomly generated point $(\hat{\tau}, \hat{\theta}) = (0.4081, 0.3969)$ for a randomly generated choice of $(\gamma_c, \gamma_s) = (0.9212, 0.8315)$. As Fig. 14 (Left) shows, the weighted centroid update is the only successful update among all the updates. Fig. 14 (Right) similarly depicts the outperformance of the weighted centroid update compared to the other updates. Also, it depicts that in the exact scenario, the other updates have attained some positive results. The descending order of the performance according to Fig. 14 (Right) is the W-centroid update, the Cheb. center update, the centroid update, and the random update. Interestingly,

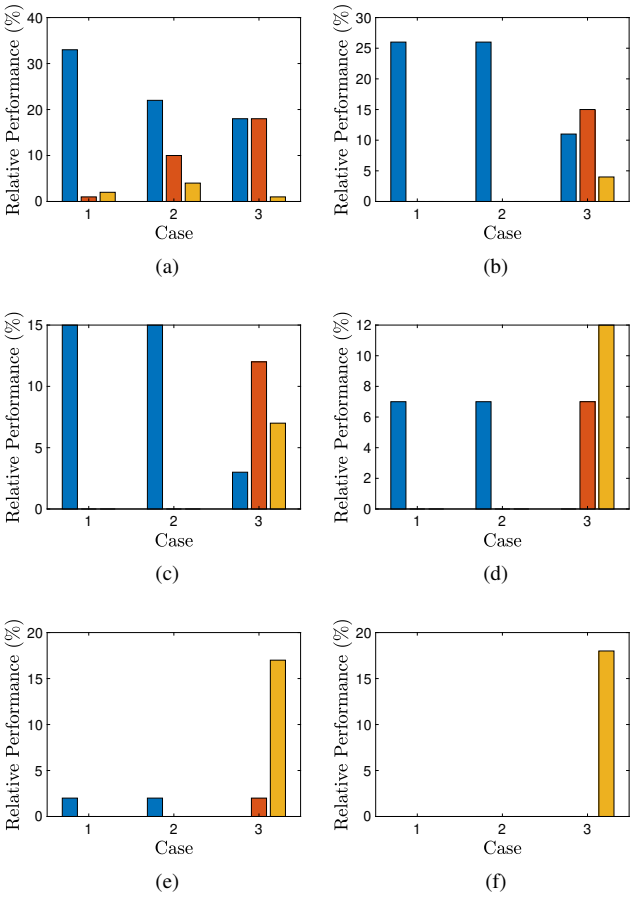

Figure 12. The relative performance of the weighted centroid update compared to the centroid update (Case 1), the Chebyshev center update (Case 2), and the update based on a point close to the origin $(\hat{\tau}, \hat{\theta}) = (0.01, 0)$ (Case 3). The Left, Middle, and Right bars in each case respectively correspond to Better, Equal, and Worse relative performances. Note that in each case the scenarios in which $\|\Delta - \hat{\Delta}\|_F < \upsilon$ holds neither by the weighted centroid update nor by the counterpart, are eliminated. (a) $(\gamma_c, \gamma_s) = (1, 1)$, (b) $(\gamma_c, \gamma_s) = (0.9, 0.9)$, (c) $(\gamma_c, \gamma_s) = (0.8, 0.8)$, (d) $(\gamma_c, \gamma_s) = (0.7, 0.7)$, (e) $(\gamma_c, \gamma_s) = (0.6, 0.6)$, and (f) $(\gamma_c, \gamma_s) = (0.5, 0.5)$.

we observe that the corresponding values of the geometric metric $\Xi_{\tau_{\hat{\Delta}}, \theta_{\hat{\Delta}}; \frac{\beta}{\rho}, n}$ (%) have the same order $(7.0944 \times 10^{-5}\%, 5.0077 \times 10^{-7}\%, 2.0450 \times 10^{-10}\%, 7.1872 \times 10^{-12}\%)$.

VI. Concluding Remarks

In this paper, we propose a simple yet efficient update of a nominal stabilizing SOF controller. According to the derived theoretical and empirical results throughout the paper, we present the following answer to the question stated in Section II (*Q1*):

A1: A least-squares problem built upon the notion of MDRP enables us to propose an efficient updated stabilizing SOF controller. For both known and unknown perturbations with a known upper bound on their norm, we derive sufficient stability conditions followed by the characterized guaranteed stability regions. Moreover, we define geometric metrics to quantify the stability robustness of the proposed updated stabilizing SOF controllers. Specifically, for unknown perturbations with a known upper bound on their norm, we interestingly observe

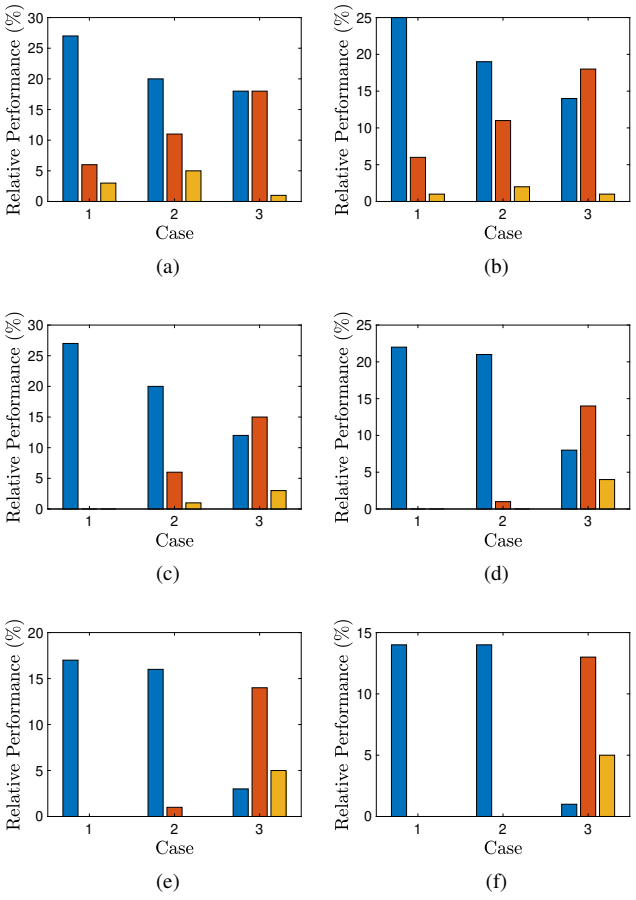

Figure 13. The relative performance of the weighted centroid update compared to the centroid update (Case 1), the Chebyshev center update (Case 2), and the update based on a point close to the origin $(\hat{\tau}, \hat{\theta}) = (0.01, 0)$ (Case 3). The Left, Middle, and Right bars in each case respectively correspond to Better, Equal, and Worse relative performances. Note that in each case the scenarios in which $\|BG^*_{\Delta} C + \Delta\|_F < \beta$ holds neither by the weighted centroid update nor by the counterpart, are eliminated. (a) $(\gamma_c, \gamma_s) = (1, 1)$, (b) $(\gamma_c, \gamma_s) = (0.9, 0.9)$, (c) $(\gamma_c, \gamma_s) = (0.8, 0.8)$, (d) $(\gamma_c, \gamma_s) = (0.7, 0.7)$, (e) $(\gamma_c, \gamma_s) = (0.6, 0.6)$, and (f) $(\gamma_c, \gamma_s) = (0.5, 0.5)$.

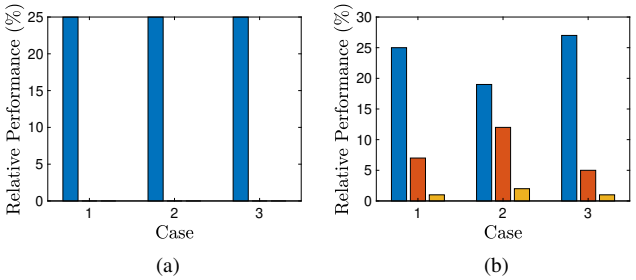

Figure 14. The relative performance of the weighted centroid update compared to the centroid update (Case 1), the Chebyshev center update (Case 2), and the update based on a randomly generated point $(\hat{\tau}, \hat{\theta}) = (0.4081, 0.3969)$ (Case 3) for a randomly generated choice of $(\gamma_c, \gamma_s) = (0.9212, 0.8315)$. The Left, Middle, and Right bars in each case respectively correspond to Better, Equal, and Worse relative performances. (a) guaranteed (conservative) scenario and (b) exact scenario.

that the NF-based robust updates attain better performance compared to the random update. Moreover, in the case of a sufficiently accurate estimation of the unknown perturbation, the descending order of the NF-based robust updates in terms of performance is the weighted centroid update, the Cheb. center update, and the centroid design.

Limitations: Like any engineering solution, the proposed updated stabilizing SOF controller has some limitations. The main limitations are three-fold: *(i)* we propose a semi-dynamic solution to a dynamic problem. The static nature comes from the utilized least-squares problem and the dynamic nature comes from the information stored in the nominal stabilizing SOF controller F for the state-space triplet (A, B, C) (i.e., $\beta_{\mathbb{R}}(A + BFC)$), *(ii)* computing the exact value of MDRP $\beta_{\mathbb{R}}(A + BFC)$ is theoretically impossible and the practical heuristics to estimate $\beta_{\mathbb{R}}(A + BFC)$ may provide the less accurate values. The less accurate $\beta_{\mathbb{R}}(A + BFC)$, the less accurate guaranteed stability we get for the proposed update. Also, the more time-consuming practical heuristics we utilize to estimate $\beta_{\mathbb{R}}(A + BFC)$, the less efficient update we get, and *(iii)* Unlike the typical update, the proposed update can be destabilizing for a subset of perturbations as illustrated by the region outside the guaranteed stability region S_κ for $\kappa < 1$, i.e., $\beta_{\mathbb{R}}(A+BFC) < \rho$. However, note that the positive point about the proposed update is that, unlike the typical update, it always provides a non-empty guaranteed stability region (the typical approach can fail to propose a updated stabilizing SOF controller as it is a sophisticated problem in general).

REFERENCES

[1] S. Barnett and C. Storey, "Insensitivity of optimal linear control systems to persistent changes in parameters," *International Journal of Control*, vol. 4, no. 2, pp. 179–184, 1966.

[2] S. Chang and T. Peng, "Adaptive guaranteed cost control of systems with uncertain parameters," *IEEE Transactions on Automatic Control*, vol. 17, no. 4, pp. 474–483, 1972.

[3] P. Wong and M. Athans, "Closed-loop structural stability for linear-quadratic optimal systems," *IEEE Transactions on Automatic Control*, vol. 22, no. 1, pp. 94–99, 1977.

[4] R. Patel, M. Toda, and B. Sridhar, "Robustness of linear quadratic state feedback designs in the presence of system uncertainty," *IEEE Transactions on Automatic Control*, vol. 22, no. 6, pp. 945–949, 1977.

[5] R. Patel and M. Toda, "Quantitative measures of robustness for multivariable systems," in *Joint Automatic Control Conference*, no. 17, 1980, p. 35.

[6] M. F. Barrett, "Conservatism with robustness tests for linear feedback control systems," in *19th IEEE Conference on Decision and Control including the Symposium on Adaptive Processes*, 1980, pp. 885–890.

[7] R. Yedavalli, "Improved measures of stability robustness for linear state space models," *IEEE Transactions on Automatic Control*, vol. 30, no. 6, pp. 577–579, 1985.

[8] R. Yedavalli and Z. Liang, "Reduced conservatism in stability robustness bounds by state transformation," *IEEE Transactions on Automatic Control*, vol. 31, no. 9, pp. 863–866, 1986.

[9] I. R. Petersen, "A stabilization algorithm for a class of uncertain linear systems," *Systems & control letters*, vol. 8, no. 4, pp. 351–357, 1987.

[10] P. P. Khargonekar, I. R. Petersen, and K. Zhou, "Robust stabilization of uncertain linear systems: quadratic stabilizability and h/sup infinity/control theory," *IEEE Transactions on Automatic control*, vol. 35, no. 3, pp. 356–361, 1990.

[11] L. Xie, M. Fu, C. E. de Souza *et al.*, "h^∞ control and quadratic stabilization of systems with parameter uncertainty via output feedback," *IEEE Transactions on Automatic Control*, vol. 37, no. 8, pp. 1253–1256, 1992.

[12] R. Arastoo, M. Bahavarnia, M. V. Kothare, and N. Motee, "Closed-loop feedback sparsification under parametric uncertainties," in *55th Conference on Decision and Control (CDC)*. IEEE, 2016, pp. 123–128.

[13] O. Toker and H. Ozbay, "On the np-hardness of solving bilinear matrix inequalities and simultaneous stabilization with static output feedback," in *Proceedings of 1995 American Control Conference-ACC'95*, vol. 4. IEEE, 1995, pp. 2525–2526.

[14] A. Majumdar, G. Hall, and A. A. Ahmadi, "Recent scalability improvements for semidefinite programming with applications in machine learning, control, and robotics," *Annual Review of Control, Robotics, and Autonomous Systems*, vol. 3, pp. 331–360, 2020.

[15] D. Henrion, J. Lofberg, M. Kocvara, and M. Stingl, "Solving polynomial static output feedback problems with penbmi," in *Proceedings of the 44th IEEE Conference on Decision and Control*, 2005, pp. 7581–7586.

[16] Q. T. Dinh, S. Gumussoy, W. Michiels, and M. Diehl, "Combining convex–concave decompositions and linearization approaches for solving bmis, with application to static output feedback," *IEEE Transactions on Automatic Control*, vol. 57, no. 6, pp. 1377–1390, 2011.

[17] C. A. Crusius and A. Trofino, "Sufficient lmi conditions for output feedback control problems," *IEEE Transactions on Automatic Control*, vol. 44, no. 5, pp. 1053–1057, 1999.

[18] C. Van Loan, "How near is a stable matrix to an unstable matrix?" Cornell University, Tech. Rep., 1984.

[19] M. Bahavarnia, C. Somarakis, and N. Motee, "State feedback controller sparsification via a notion of non-fragility," in *56th Annual Conference on Decision and Control (CDC)*. IEEE, 2017, pp. 4205–4210.

[20] M. Bahavarnia, "State-feedback controller sparsification via quasi-norms," in *American Control Conference (ACC)*. IEEE, 2019, pp. 748–753.

[21] R. A. Horn and C. R. Johnson, *Matrix analysis*. Cambridge university press, 2012.

[22] D. Hinrichsen and A. J. Pritchard, "Stability radii of linear systems," *Systems & Control Letters*, vol. 7, no. 1, pp. 1–10, 1986.

[23] ——, "Real and complex stability radii: a survey," in *Control of Uncertain Systems: Proceedings of an International Workshop Bremen, West Germany, June 1989*. Springer, 1990, pp. 119–162.

[24] S. Boyd and L. Vandenberghe, *Convex optimization*. Cambridge university press, 2004.

[25] M. A. Rahimian and M. S. Tavazoei, "Constrained tuning of two-parameter controllers: a centroid approach," *Proceedings of the Institution of Mechanical Engineers, Part I: Journal of Systems and Control Engineering*, vol. 226, no. 5, pp. 685–698, 2012.

[26] ——, "Application of stability region centroids in robust pi stabilization of a class of second-order systems," *Transactions of the Institute of Measurement and Control*, vol. 34, no. 4, pp. 487–498, 2012.

[27] M. Bahavarnia and M. S. Tavazoei, "A new view to ziegler–nichols step response tuning method: Analytic non-fragility justification," *Journal of Process Control*, vol. 23, no. 1, pp. 23–33, 2013.

[28] ——, "A probabilistic framework to achieve robust non-fragile tuning methods: Pd control of ipd-modeled processes," *International Journal of Robust and Nonlinear Control*, vol. 32, no. 18, pp. 9593–9609, 2022.

[29] S. Li, "Concise formulas for the area and volume of a hyperspherical cap," *Asian Journal of Mathematics & Statistics*, vol. 4, no. 1, pp. 66–70, 2011.

[30] F. Leibfritz, "Compleib: Constrained matrix optimization problem library," 2006.

[31] P. Gahinet and P. Apkarian, "Structured $\mathcal{H}_\infty$ synthesis in matlab," *IFAC Proceedings Volumes*, vol. 44, no. 1, pp. 1435–1440, 2011.

[32] P. Apkarian and D. Noll, "Nonsmooth h^∞ synthesis," *IEEE Transactions on Automatic Control*, vol. 51, no. 1, pp. 71–86, 2006.

[33] R. Harman and V. Lacko, "On decompositional algorithms for uniform sampling from n-spheres and n-balls," *Journal of Multivariate Analysis*, vol. 101, no. 10, pp. 2297–2304, 2010.

[34] T. M. Apostol, *Calculus, volume 1*. John Wiley & Sons, 1991.

APPENDIX A
PROOF OF LEMMA 1

Considering $\Sigma_H = \begin{bmatrix}\Gamma_H^T & 0\end{bmatrix}^T$ and noting that $U_H^T U_H = I_{n^2}$ and $V_H^T V_H = I_{mp}$ hold, we have

$$
\begin{aligned}
&P := I_{n^2} - HH^+ = I_{n^2} - H(H^TH)^{-1}H^T = \\
&I_{n^2} - U_H\Sigma_H V_H^T (V_H\Sigma_H^T U_H^T U_H \Sigma_H V_H^T)^{-1} V_H \Sigma_H^T U_H^T = \\
&I_{n^2} - U_H\Sigma_H V_H^T (V_H(\Gamma_H^2)^{-1}V_H^T) V_H \Sigma_H^T U_H^T = \\
&I_{n^2} - U_H \begin{bmatrix}\Gamma_H^T & 0\end{bmatrix}^T (\Gamma_H^2)^{-1} \begin{bmatrix}\Gamma_H^T & 0\end{bmatrix} U_H^T = \\
&U_H I_{n^2} U_H^T - U_H \begin{bmatrix} I_{mp} & 0 \\ 0 & 0\end{bmatrix} U_H^T = U_H \begin{bmatrix} 0 & 0 \\ 0 & I_{n^2-mp}\end{bmatrix} U_H^T.
\end{aligned}
$$

Moreover, according to $H := C^T \otimes B$ and the properties of Kronecker product, we get

$$
\begin{aligned}
H := C^T \otimes B = (V_C \otimes U_B)(\Sigma_C^T \otimes \Sigma_B)(U_C \otimes V_B)^T = \\
(V_C \otimes U_B)(U_\Omega \Sigma_\Omega V_\Omega^T)(U_C \otimes V_B)^T = \\
((V_C \otimes U_B)U_\Omega)\Sigma_\Omega((U_C \otimes V_B)V_\Omega)^T.
\end{aligned}
$$

Then, we have

$$
(U_H, \Sigma_H, V_H) = ((V_C \otimes U_B)U_\Omega, \Sigma_\Omega, (U_C \otimes V_B)V_\Omega),
$$

which completes the proof.

APPENDIX B
PROOF OF PROPOSITION 1

Substituting (15) of Lemma 1 in (14), we get

$$
\begin{aligned}
J^*(\Delta) = \mathbf{vec}(\Delta)^T U_H \begin{bmatrix} 0 & 0 \\ 0 & I_{n^2-mp}\end{bmatrix} U_H^T \mathbf{vec}(\Delta) = \\
\delta^T U_H \begin{bmatrix} 0 & 0 \\ 0 & I_{n^2-mp}\end{bmatrix} U_H^T \delta.
\end{aligned}
$$

Then, defining $\chi := U_H^T\delta$ and noting that $U_H^T U_H = I_{n^2}$ holds, we get $\delta = U_H\chi$. Since $\delta^T\delta = \chi^T U_H^T U_H \chi$, $U_H^T U_H = I_{n^2}$, and $\delta^T\delta = \|\Delta\|_F^2 = r^2$ hold, we get $\chi^T\chi = r^2$ that inspires us to define $\psi := \frac{\chi}{\|\chi\|} = \frac{\chi}{r}$. Note that $\psi \in \mathbb{R}^{n^2}$ and $\|\psi\| = 1$ hold. Then, we have $\chi = r\psi$ and subsequently we get $\delta = U_H\chi = rU_H\psi$. Defining $\mu \in \mathbb{R}^{mp}$ and $\nu \in \mathbb{R}^{n^2-mp}$ as follows:

$$
\mu := \begin{bmatrix} I_{mp} & 0\end{bmatrix}\psi, \nu := \begin{bmatrix} 0 & I_{n^2-mp}\end{bmatrix}\psi,
$$

we get $\psi = \begin{bmatrix}\mu^T & \nu^T\end{bmatrix}^T$. Since $\|\psi\|^2 = \|\mu\|^2 + \|\nu\|^2 = 1$ holds, we can consider $\|\mu\| = \cos(\frac{\pi\theta}{2})$ and $\|\nu\| = \sin(\frac{\pi\theta}{2})$ for a $\theta \in [0,1]$. Then, we have

$$
\mu = \frac{\mu}{\|\mu\|}\cos\left(\frac{\pi\theta}{2}\right), \nu = \frac{\nu}{\|\nu\|}\sin\left(\frac{\pi\theta}{2}\right).
$$

Defining $\phi_c := \frac{\mu}{\|\mu\|}$ and $\phi_s := \frac{\nu}{\|\nu\|}$, we get $\mu = \phi_c\cos(\frac{\pi\theta}{2})$ and $\nu = \phi_s\sin(\frac{\pi\theta}{2})$ (Note that $\|\phi_c\| = 1$ and $\|\phi_s\| = 1$ hold). Then, considering the $r = \rho\sin(\frac{\pi\tau}{2})$ with $\tau \in]0,1]$, we have

$$
\begin{aligned}
\Delta = \mathbf{vec}^{-1}(\delta) = \mathbf{vec}^{-1}(rU_H\psi) = \\
r\mathbf{vec}^{-1}\left((V_C \otimes U_B)U_\Omega \begin{bmatrix}\phi_c\cos(\frac{\pi\theta}{2}) \\ \phi_s\sin(\frac{\pi\theta}{2})\end{bmatrix}\right) = \\
\rho\sin\left(\frac{\pi\tau}{2}\right)U_B\mathbf{vec}^{-1}\left(U_\Omega \begin{bmatrix}\phi_c\cos(\frac{\pi\theta}{2}) \\ \phi_s\sin(\frac{\pi\theta}{2})\end{bmatrix}\right)V_C^T.
\end{aligned}
$$

which completes the proof of (16).

Also, for $J^*(\Delta)$ in (14), we have

$$
\begin{aligned}
&J^*(\Delta) = \mathbf{vec}(\Delta)^T P \mathbf{vec}(\Delta) = \delta^T P \delta = (rU_H\psi)^T P (rU_H\psi) \\
&r^2\psi^T U_H^T P U_H \psi = r^2 \begin{bmatrix}\mu^T & \nu^T\end{bmatrix} \begin{bmatrix} 0 & 0 \\ 0 & I_{n^2-mp}\end{bmatrix} \begin{bmatrix}\mu \\ \nu\end{bmatrix} = \\
&r^2\nu^T\nu = r^2\left(\phi_s\sin\left(\frac{\pi\theta}{2}\right)\right)^T\phi_s\sin\left(\frac{\pi\theta}{2}\right) = \\
&\left(r\sin\left(\frac{\pi\theta}{2}\right)\right)^2\|\phi_s\|^2 = \left(\rho\sin\left(\frac{\pi\tau}{2}\right)\sin\left(\frac{\pi\theta}{2}\right)\right)^2,
\end{aligned}
$$

which completes the proof of (17).

APPENDIX C
PROOF OF PROPOSITION 2

We use (4) as a sufficient condition on the stability of the updated perturbed state-space (3). By substituting G^*_Δ in (4), we get

$$\sin\left(\frac{\pi\tau}{2}\right)\sin\left(\frac{\pi\theta}{2}\right) < \frac{\beta_{\mathbb{R}}(A+BFC)}{\rho}. \tag{43}$$

If $\rho < \beta_{\mathbb{R}}(A+BFC)$ holds, then $F + G^*_\Delta$ with G^*_Δ in (12) is an updated stabilizing SOF controller because the left-hand-side of (43) is at most 1 and the right-hand-side of (43) is greater than 1. Then, (43) holds.

If $\rho \geq \beta_{\mathbb{R}}(A+BFC)$ holds, since $\sin(\frac{\pi\theta}{2})$ attains its maximum value at $\theta = 1$, (43) reduces to

$$\sin\left(\frac{\pi\tau}{2}\right) < \frac{\beta_{\mathbb{R}}(A+BFC)}{\rho},$$

or equivalently

$$\tau < \frac{2}{\pi}\arcsin\left(\frac{\beta_{\mathbb{R}}(A+BFC)}{\rho}\right),$$

from which, we define κ in (18). Similarly, we may extract the definition of $\zeta_{\tau,\kappa}$ in (18). Thus, if $(\tau_\Delta, \theta_\Delta) \in S_\kappa$ holds, then $F + G^*_\Delta$ with G^*_Δ in (12) is an updated stabilizing SOF controller.

The expression in (19) expresses the area of S_κ divided by the area of unit square $]0,1] \times [0,1]$ in 2-dimensional parametric space of (τ, θ). Note that $\int_0^\kappa 1 d\tau = \kappa$ has simplified the right-hand-side of (19). To show that ξ_κ is an increasing function of κ, we compute the derivative of ξ_κ with respect to κ as follows (utilizing the Leibniz integral rule [34]):

$$\frac{d\xi_\kappa}{d\kappa} = \cos\left(\frac{\pi\kappa}{2}\right)\int_\kappa^1 \frac{1}{\sqrt{\sin(\frac{\pi\tau}{2})^2 - \sin(\frac{\pi\kappa}{2})^2}} d\tau. \tag{44}$$

According to (44), $\frac{d\xi_\kappa}{d\kappa} \geq 0$ holds and noting that

$$\frac{d\kappa}{d\rho} = -\frac{2\beta}{\pi\rho\sqrt{\rho^2-\beta^2}} < 0, \frac{d\kappa}{d\beta} = \frac{2}{\pi\sqrt{\rho^2-\beta^2}} > 0,$$

hold, the proof is complete.

APPENDIX D
PROOF OF PROPOSITION 3

On the one hand, using (4) as a sufficient condition on the stability of the updated perturbed state-space (3) and substituting $G^*_{\hat\Delta}$ in (4), we get

$$\|BG^*_{\hat\Delta}C + \Delta\|_F < \beta_{\mathbb{R}}(A+BFC). \tag{45}$$

On the other hand, by applying the triangle inequality, we get

$$\|BG^*_{\hat\Delta}C + \Delta\|_F \leq \|BG^*_{\hat\Delta}C + \hat\Delta\|_F + \|\Delta - \hat\Delta\|_F. \tag{46}$$

Considering (45) and (46), we derive the following sufficient condition:

$$\|\Delta - \hat\Delta\|_F < \beta_{\mathbb{R}}(A+BFC) - \|BG^*_{\hat\Delta}C + \hat\Delta\|_F. \tag{47}$$

Substituting $\|BG^*_{\hat\Delta}C + \hat\Delta\|_F = \rho\sin(\frac{\pi\tau_{\hat\Delta}}{2})\sin(\frac{\pi\theta_{\hat\Delta}}{2})$ in (47), we get (22). Since $\|\Delta - \hat\Delta\|_F \geq 0$ holds, the satisfaction of (22) implies that $\upsilon > 0$ must hold. In the case of $\rho < \beta_{\mathbb{R}}(A+BFC)$, it automatically holds because $(\tau_{\hat\Delta}, \theta_{\hat\Delta}) \in \hat{\mathbb{S}}$ holds and in the case of $\rho \geq \beta_{\mathbb{R}}(A+BFC)$, it holds if and only if $(\tau_{\hat\Delta}, \theta_{\hat\Delta}) \in \hat S_\kappa$ holds which completes the proof.

APPENDIX E
PROOF OF LEMMA 2

Noting that $U_H^T U_H = I_{n^2}$ and $\|\psi\| = 1$, $\|\hat\psi\| = 1$, and $\psi^T\hat\psi = \|\psi\|\|\hat\psi\|\cos(\pi\eta)$ hold, we have

$$\|\Delta - \hat\Delta\|_F^2 = \|\delta - \hat\delta\|^2 = \|\rho s_\tau U_H\psi - \rho s_{\hat\tau}U_H\hat\psi\|^2 =$$
$$\rho^2(s_\tau U_H\psi - s_{\hat\tau}U_H\hat\psi)^T(s_\tau U_H\psi - s_{\hat\tau}U_H\hat\psi) =$$
$$\rho^2(s_\tau^2 + s_{\hat\tau}^2 - 2s_\tau s_{\hat\tau}\psi^T\hat\psi) = \rho^2(s_\tau^2 + s_{\hat\tau}^2 - 2s_\tau s_{\hat\tau}c_{2\eta}).$$

which ends the proof taking the square root of both sides.

APPENDIX F
PROOF OF PROPOSITION 4

Utilizing the results of Proposition 3 and Lemma 2, and dividing the both sides of (22) by $\rho s_{\hat\tau}$, we get

$$\sqrt{\frac{1}{s_{\hat\tau}^2}s_\tau^2 + 1 - \frac{2c_{2\eta}}{s_{\hat\tau}}s_\tau} < \iota. \tag{48}$$

Then, $0 < \iota$ must hold. Assuming that $0 < \iota$ holds, squaring the both sides of (48) and multiplying the both sides by $s_{\hat\tau}^2$, we obtain the following quadratic inequality (in terms of s_τ):

$$s_\tau^2 - 2s_{\hat\tau}c_{2\eta}s_\tau + s_{\hat\tau}^2(1-\iota^2) < 0. \tag{49}$$

Observe that (49) holds if and only if

$$b_l(\eta) < s_\tau < b_u(\eta), \tag{50}$$

holds for which $s_{2\eta} < \iota$ must hold. Since $0 < s_\tau$ holds, then $0 < b_u(\eta)$ must hold based on (50). Moreover, it can be verified that the following equivalence holds:

$$0 < b_u(\eta) \iff \iota > 1 \vee \left(0 < \iota \leq 1 \wedge 0 \leq \eta < \frac{1}{2}\right). \tag{51}$$

In the case of $0 < \iota \leq 1$, $s_{2\eta} < \iota$ is equivalent to $0 \leq \eta < \bar\eta$ as $\arcsin(\pi\eta)$ is an increasing function of η for $0 \leq \eta < \frac{1}{2}$ (according to (51)) and in the case of $\iota > 1$, observe that $s_{2\eta} < \iota$ automatically holds as $s_{2\eta} \leq 1$ is satisfied. Then, these observations can compactly be expressed as

$$s_{2\eta} < \iota \iff \big(\iota > 1 \vee (0 < \iota \leq 1 \wedge 0 \leq \eta < \bar\eta)\big). \tag{52}$$

Under the $b_u(\eta) > 1$, observe that $s_\tau < b_u(\eta)$ in (50) automatically holds as $s_\tau \leq 1$ is satisfied. Moreover, it can be verified that the following equivalence holds:

$$b_u(\eta) \leq 1 \iff c_{2\eta} \leq \hat b. \tag{53}$$

Also, based on $|\hat b|$, (53) can equivalently be expressed as

$$b_u(\eta) \leq 1 \iff \Big(\hat b > 1 \vee \big(|\hat b| \leq 1 \wedge \eta \geq \underline{\eta}\big)\Big). \tag{54}$$

Under the $b_l(\eta) < 0$, observe that $b_l(\eta) < s_\tau$ in (50) automatically holds as $0 < s_\tau$ is satisfied. Moreover, it can be verified that the following equivalence holds:

$$0 \leq b_l(\eta) \iff \left(0 < \iota \leq 1 \wedge 0 \leq \eta < \frac{1}{2}\right). \tag{55}$$

It is noteworthy that for the case of $0 < \iota \leq 1$

$$0 < \bar\eta \leq \frac{1}{2}, \tag{56}$$

holds. Also, for the case of $0 < \iota \leq 1$ and $|\hat{b}| \leq 1$

$$\underline{\eta} < \bar{\eta}, \tag{57}$$

holds. To prove that, we have

$$\frac{1}{\pi}\arccos(\hat{b}) < \frac{1}{\pi}\arcsin(\iota) \iff \sqrt{1-\iota^2} < \hat{b},$$

where $\sqrt{1-\iota^2} < \hat{b}$ is satisfied according to the arithmetic-geometric inequality as

$$\sqrt{1-\iota^2} \leq \frac{s_{\hat{\tau}}(1-\iota^2) + \frac{1}{s_{\hat{\tau}}}}{2},$$

where the equality cannot occur as $s_{\hat{\tau}}(1-\iota^2) < 1 \leq \frac{1}{s_{\hat{\tau}}}$ holds.

Case i. According to (50)-(52) and (54)-(57), $\mathcal{S}$ in (24) can be defined.

Case ii. According to (50)-(52) and (54)-(56), $\mathcal{S}$ in (25) can be defined.

Case iii. According to (50)-(52), (54), and (55), $\mathcal{S}$ in (26) can be defined.

Case iv. According to (50)-(52), (54), and (55), $\mathcal{S}$ in (27) can be defined.

Case v. According to (50)-(52), (54), and (55), $\mathcal{S}$ in (28) can be defined which ends the proof.